Supplementary Information for

High molecular weight PE elastomers through 4,4-difluorobenzhydryl substitution in symmetrical α-diimino-nickel ethylene polymerization catalysts

Yuting Zheng,[a,b] Shu Jiang,[a,b] Ming Liu,[b] Zhixin Yu,*[,a] Yanping Ma,[b,c] Gregory A. Solan, *[,b,c] Wenjuan Zhang,[b,d] Tongling Liang,[b] Wen-Hua Sun *[,b]

[a] School of Pharmaceutical Sciences, Changchun University of Chinese Medicine, Changchun 130117, China.

[b] Key Laboratory of Engineering Plastics and Beijing National Laboratory for Molecular Sciences, Institute of Chemistry, Chinese Academy of Sciences, Beijing 100190, China.

[c] Department of Chemistry, University of Leicester, University Road, Leicester LE1 7RH, UK.

[d] Beijing Key Laboratory of Clothing Materials R&D and Assessment, Beijing Engineering Research Center of Textile Nanofiber, School of Materials Science and Engineering, Beijing Institute of Fashion Technology, Beijing 100029, China.

Table of contents page

^{1}H NMR (400 MHz, $CDCl_3$, 25 °C) spectra

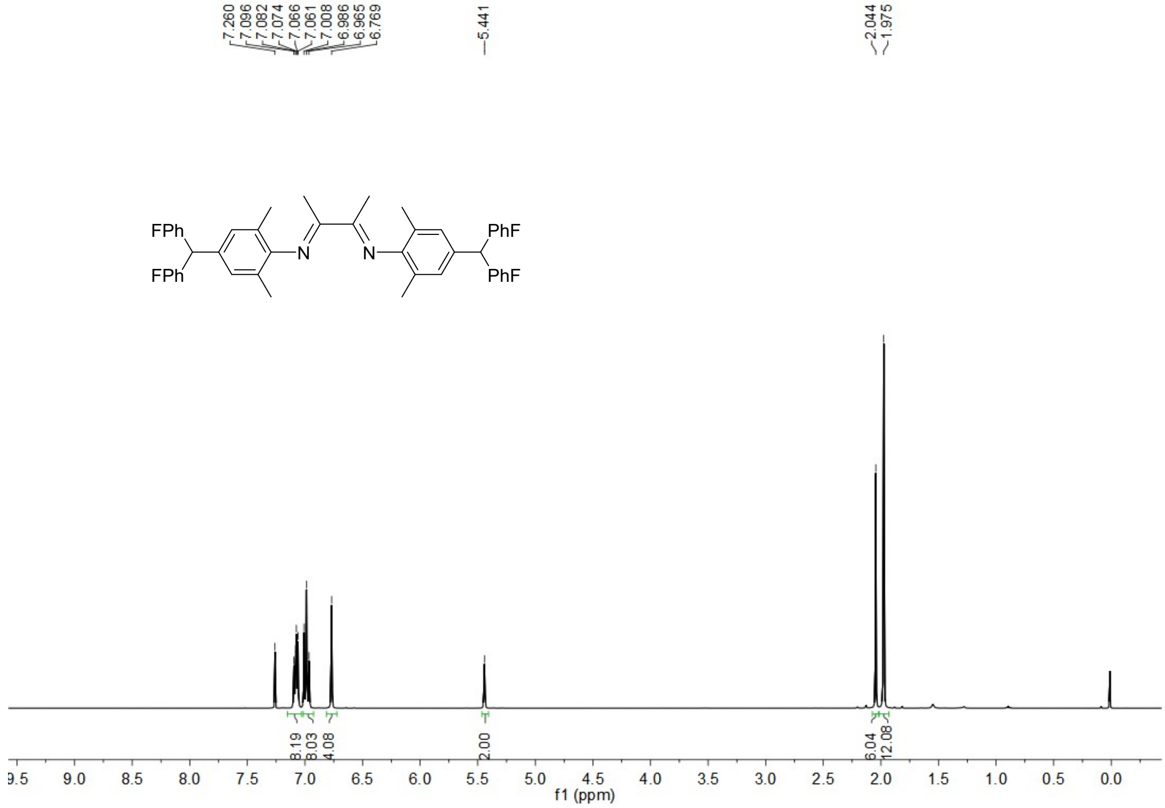

Figure S1 ^{1}H NMR spectrum of **L1**

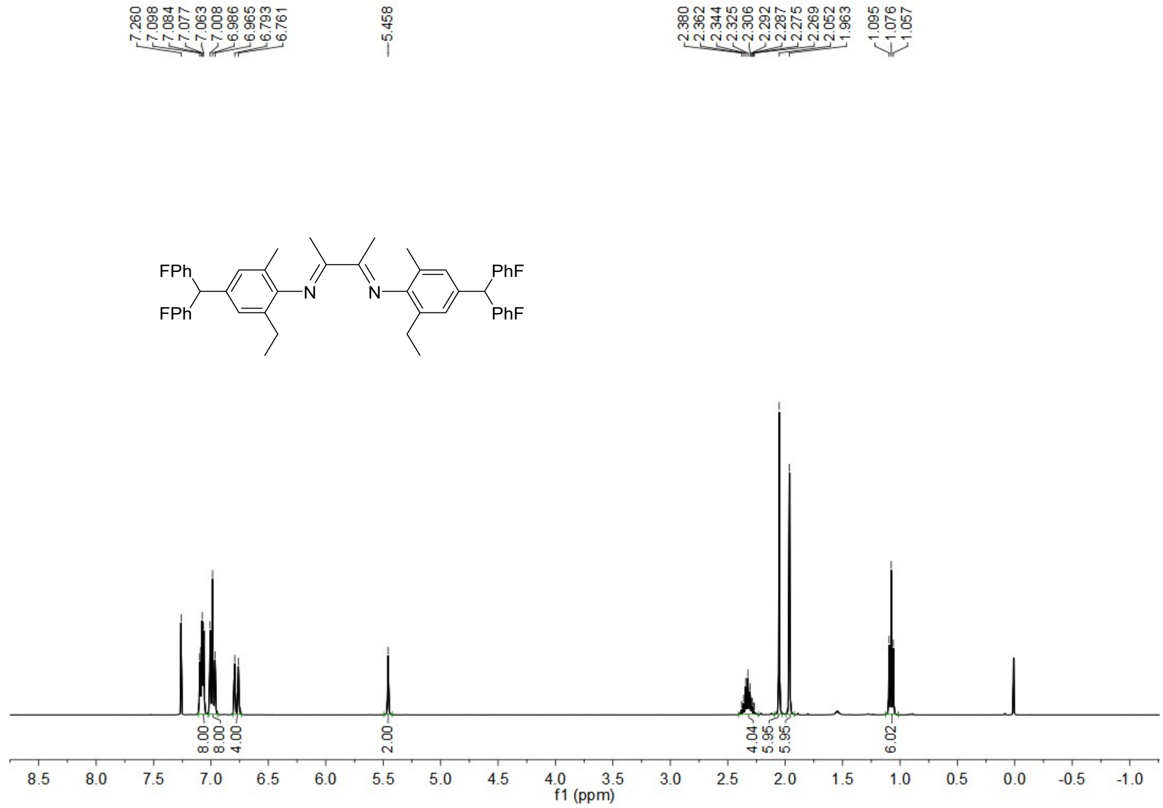

Figure S2 ^{1}H NMR spectrum of **L2**

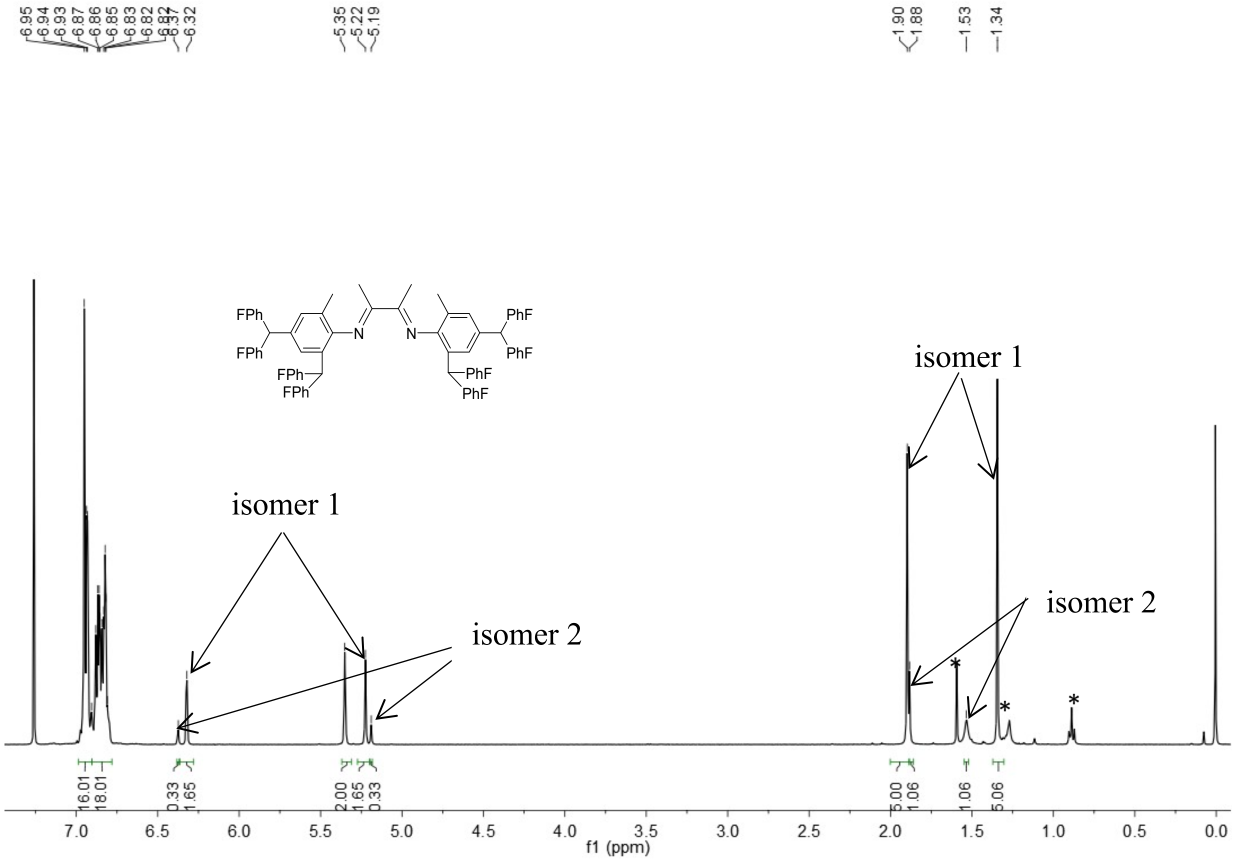

Figure S3 ^{1}H NMR spectrum of **L3**; * refers to δH for water and n-hexane

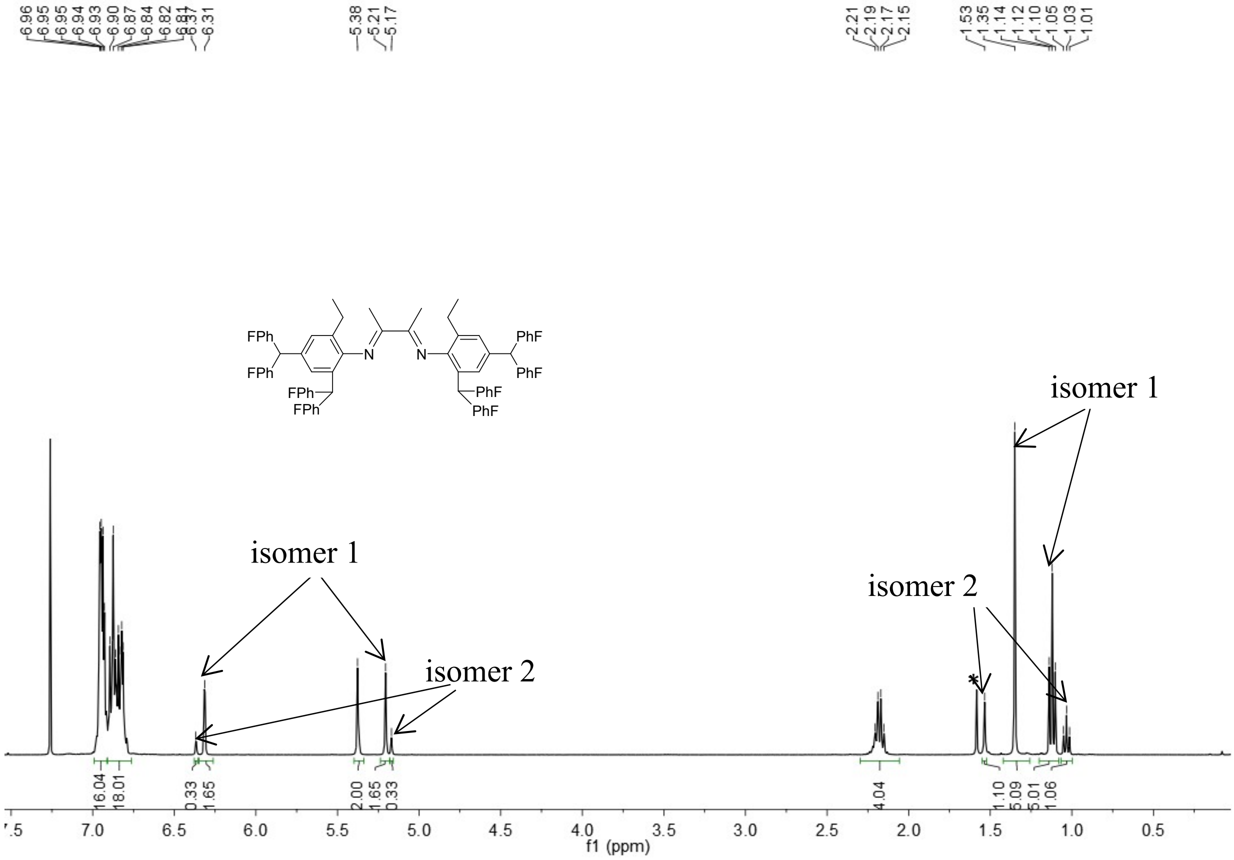

Figure S4 ^{1}H NMR spectrum of **L4**; * refers to δH for water

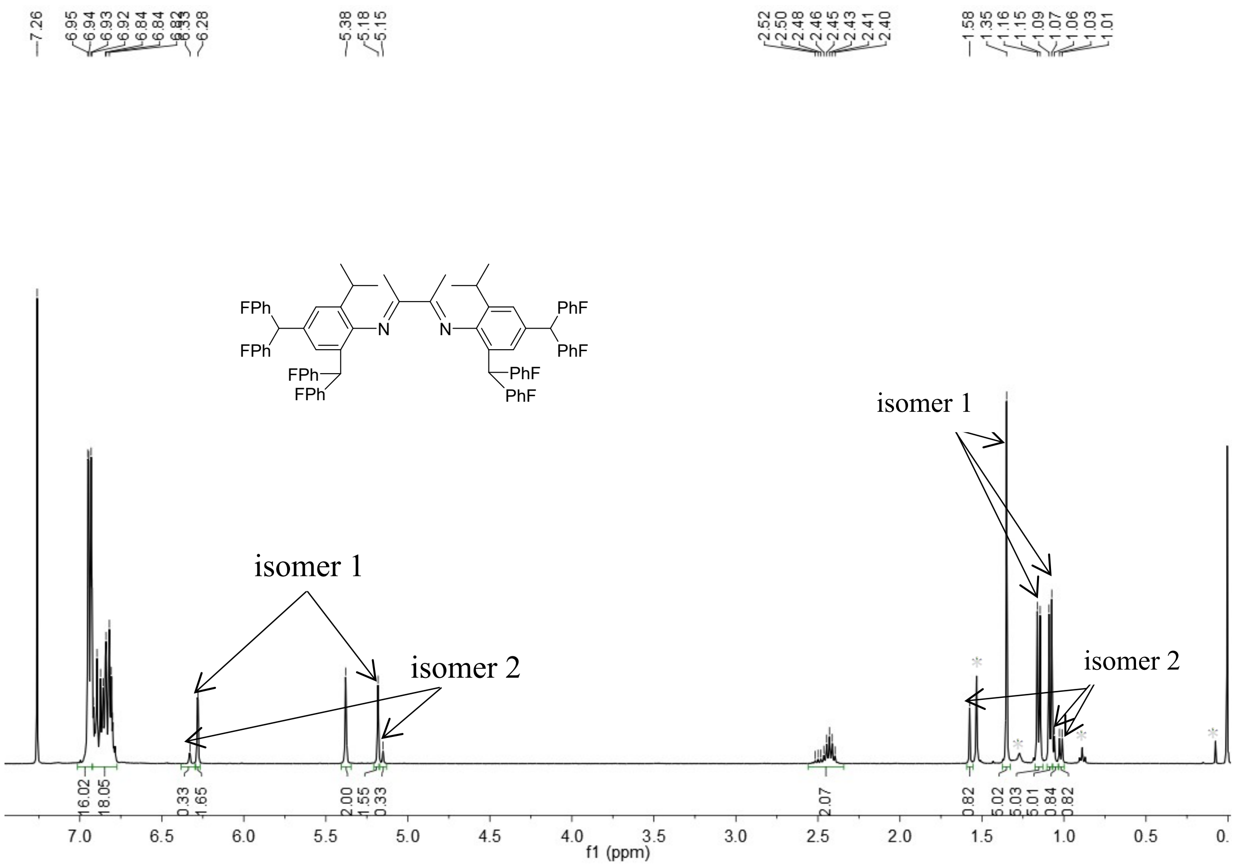

Figure S5 ^{1}H NMR spectrum of **L5**; * refers to δH for water, n-hexane and grease.

^{13}C NMR (100 MHz, $CDCl_3$, 25 °C) spectra

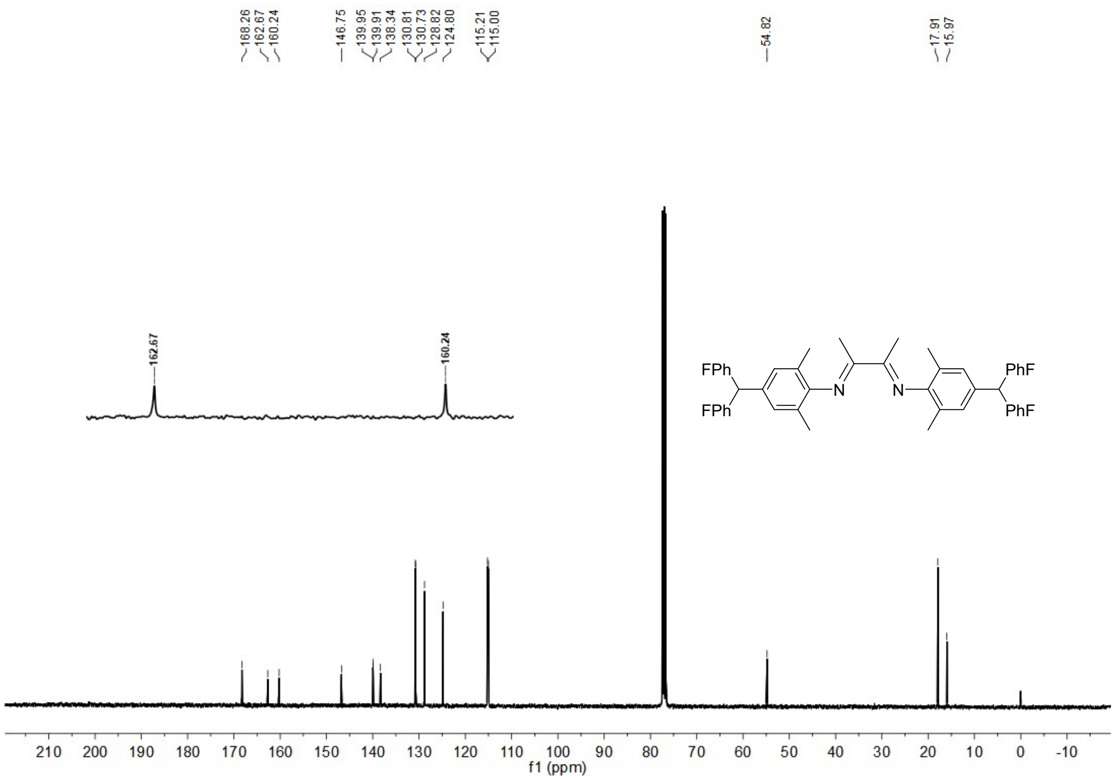

Figure S6 ^{13}C NMR spectrum of **L1**

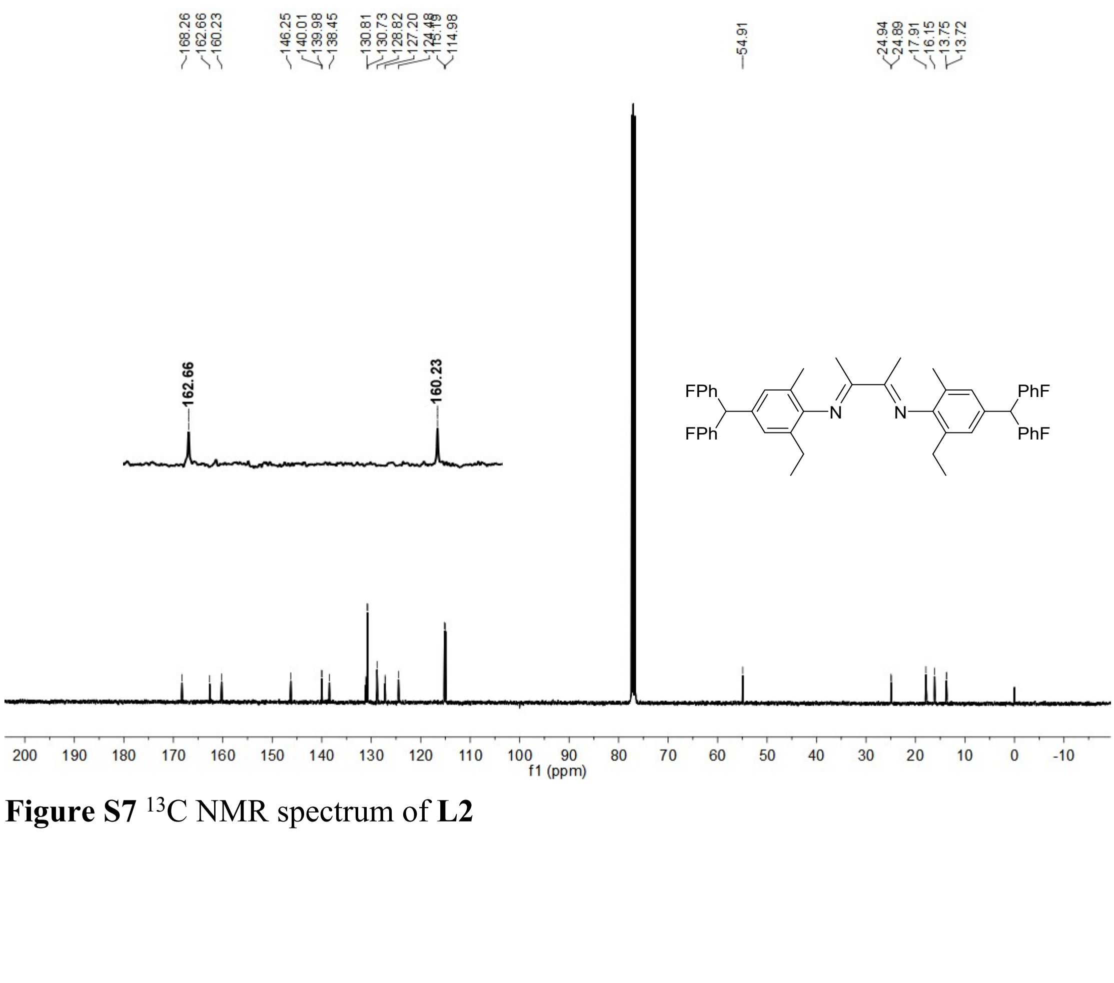

Figure S7 ^{13}C NMR spectrum of **L2**

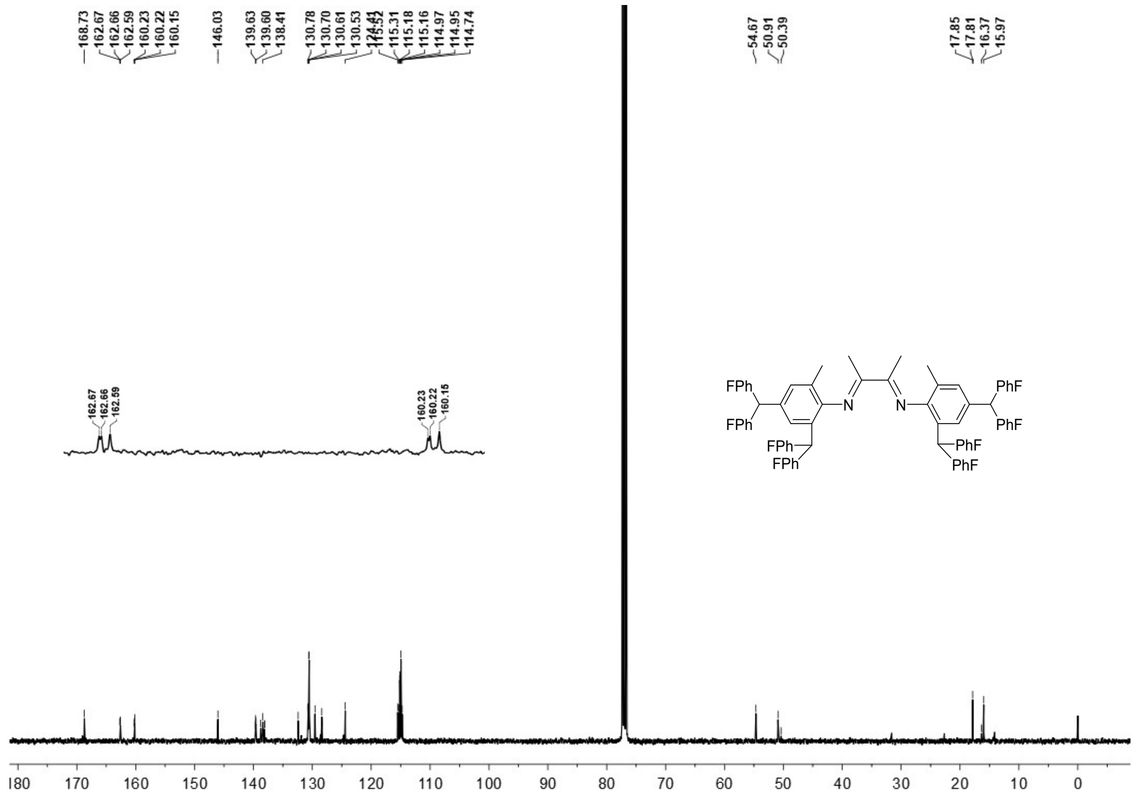

Figure S8 ^{13}C NMR spectrum of **L3**

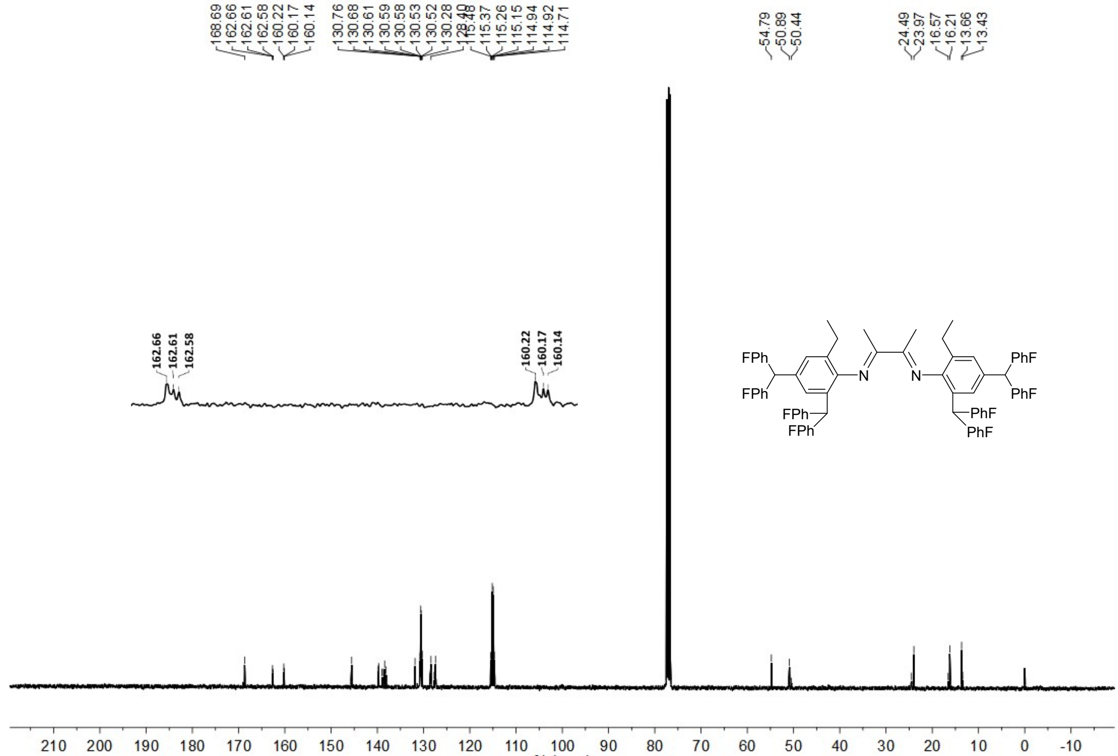

Figure S9 ^{13}C NMR spectrum of **L4**

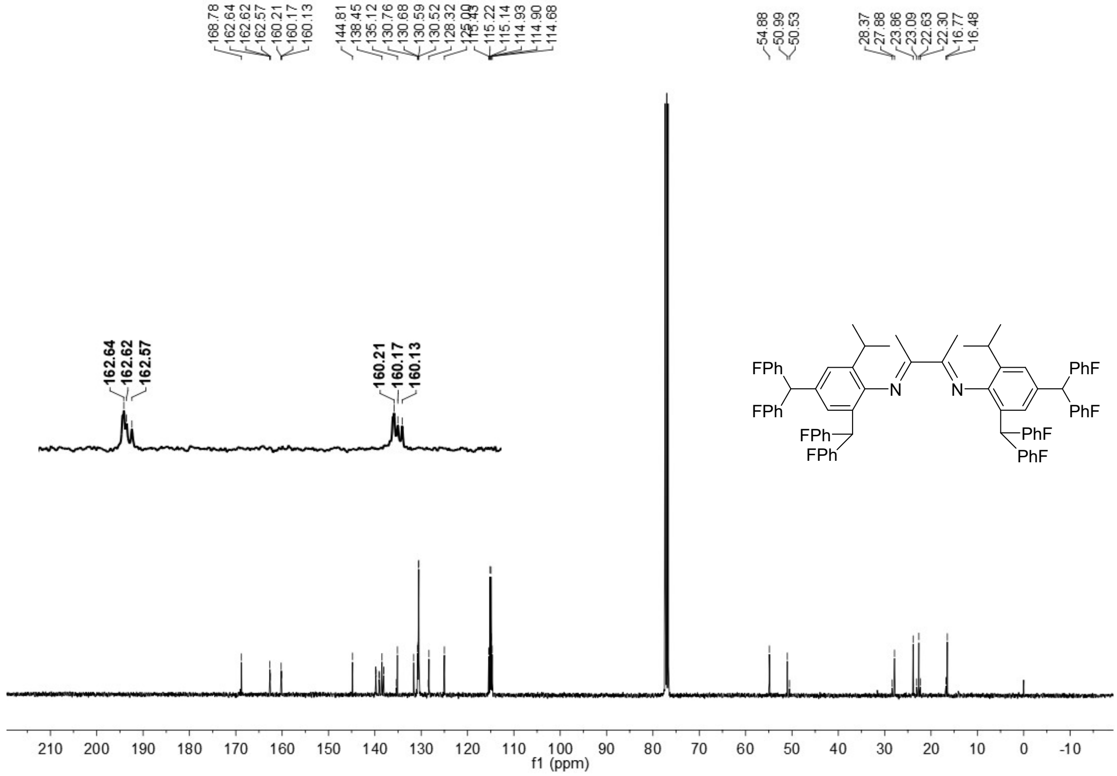

Figure S10 ^{13}C NMR spectrum of **L5**

FT-IR spectra

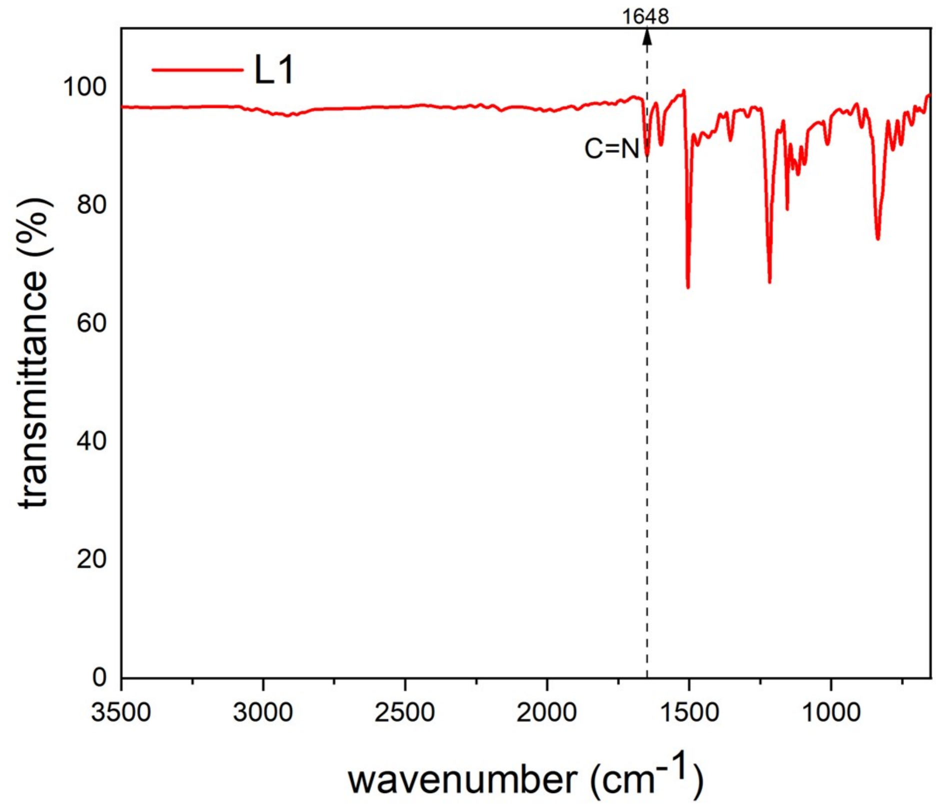

Figure S11 FT-IR spectrum of **L1**

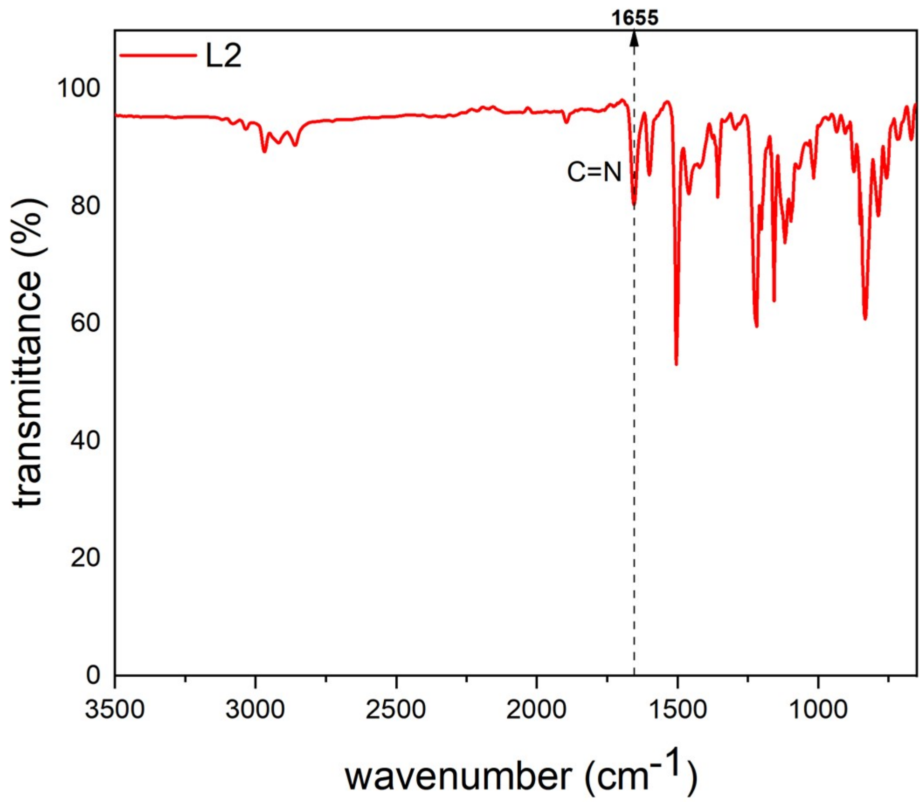

Figure S12 FT-IR spectrum of **L2**

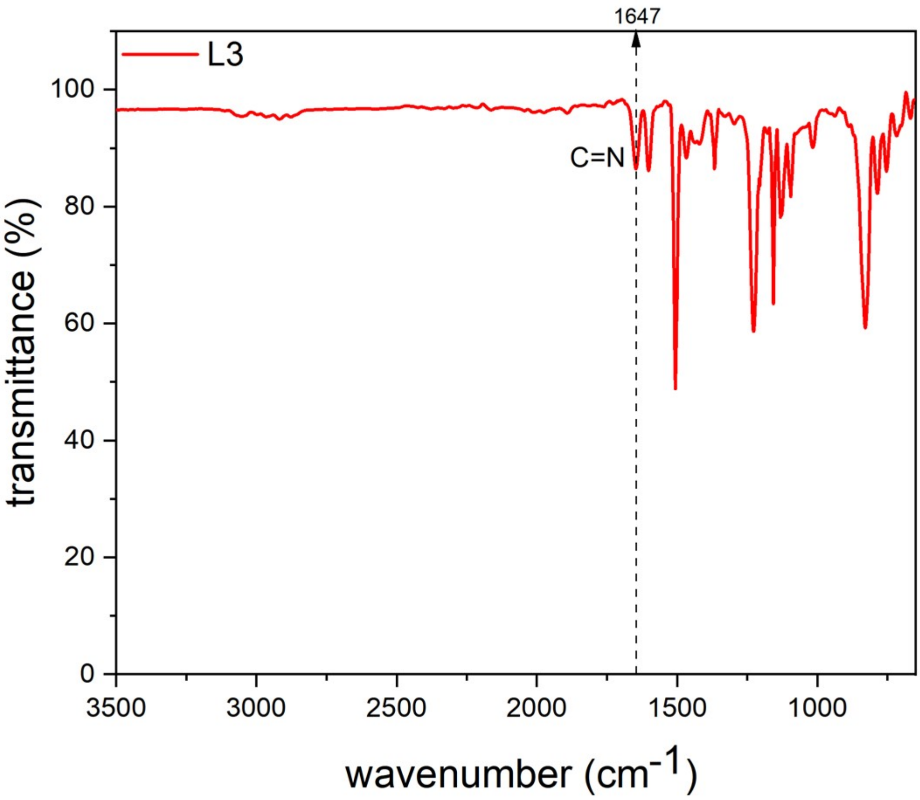

Figure S13 FT-IR spectrum of **L3**

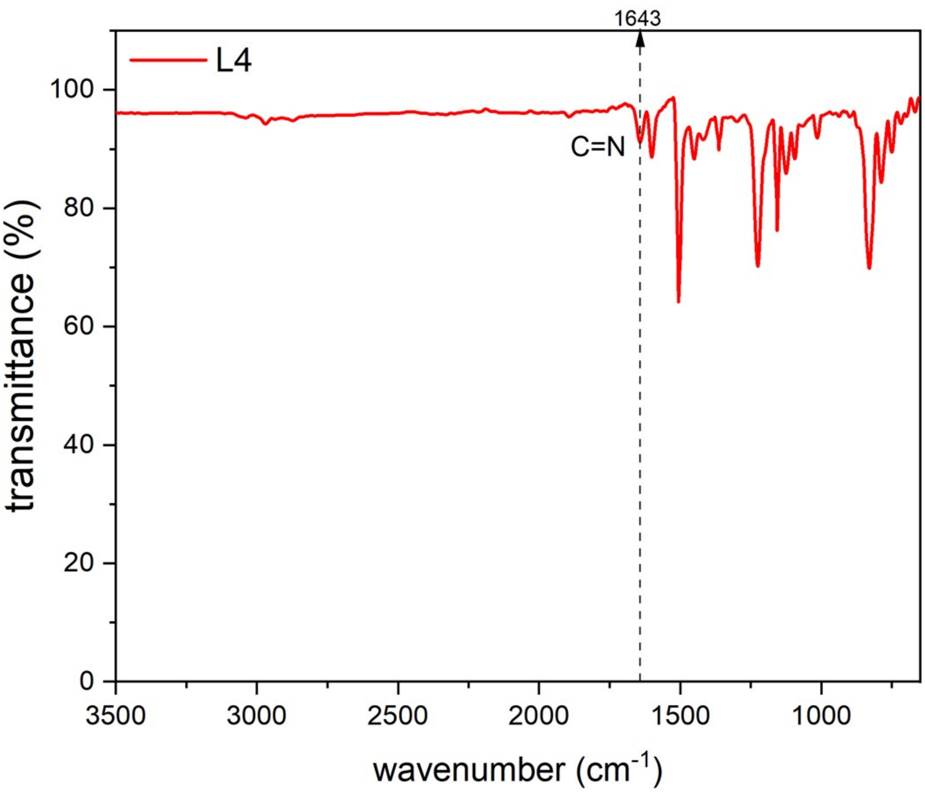

Figure S14 FT-IR spectrum of **L4**

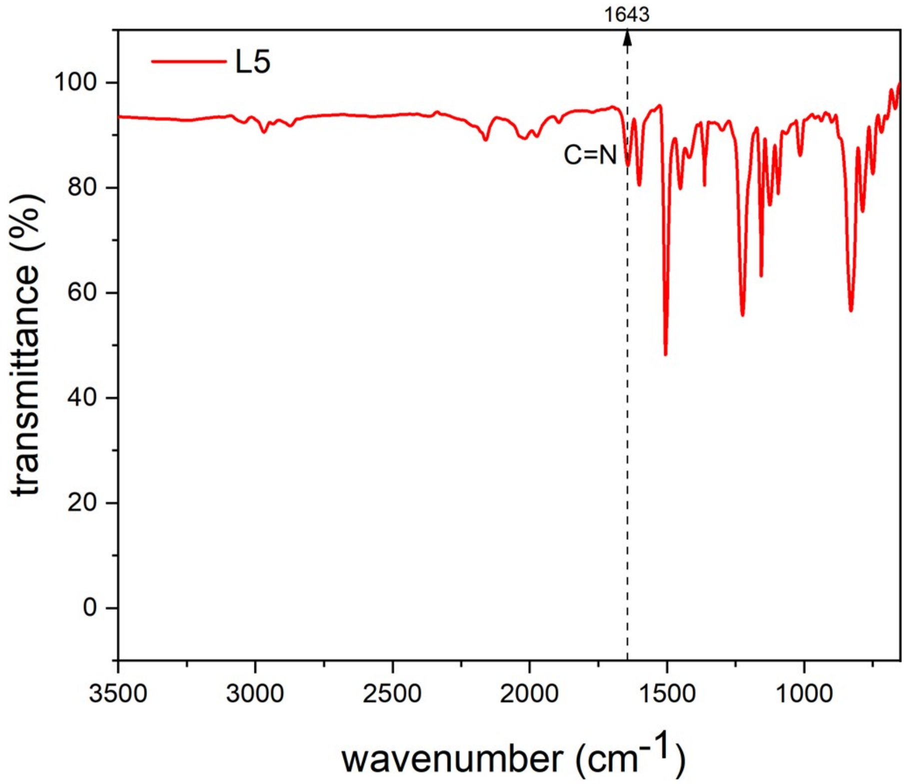

Figure S15 FT-IR spectrum of **L5**

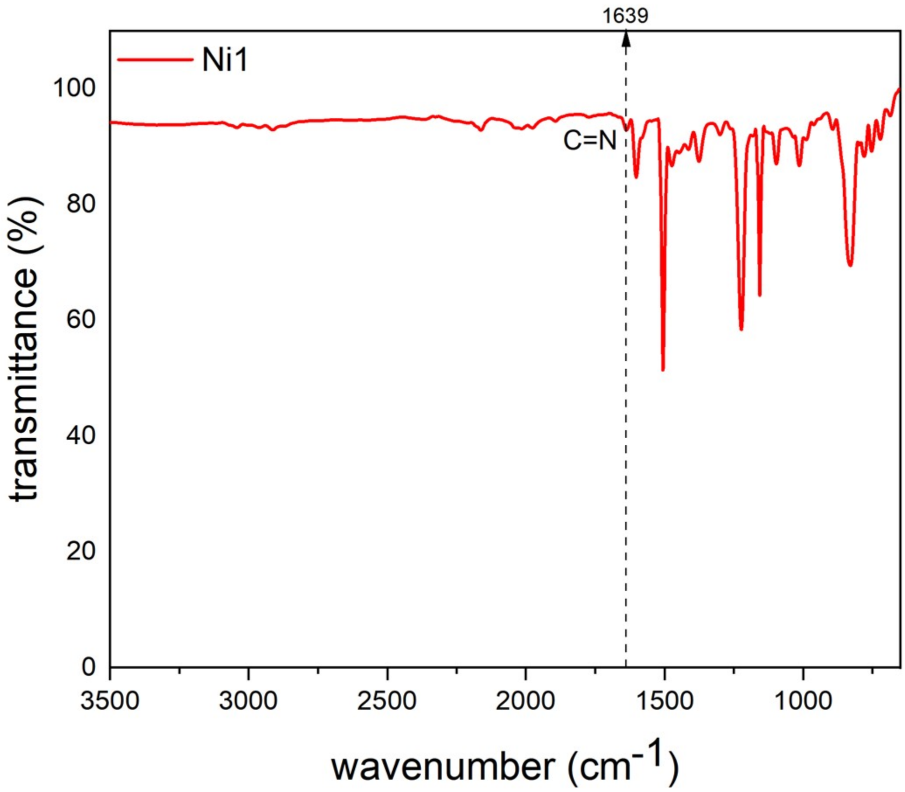

Figure S16 FT-IR spectrum of **Ni1**

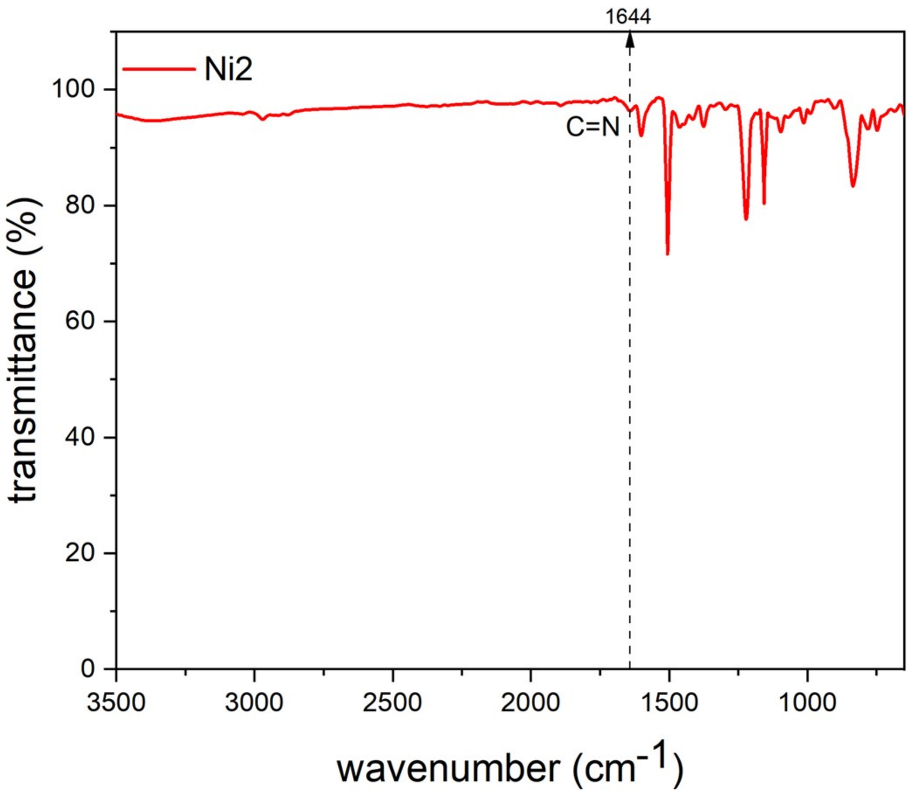

Figure S17 FT-IR spectrum of **Ni2**

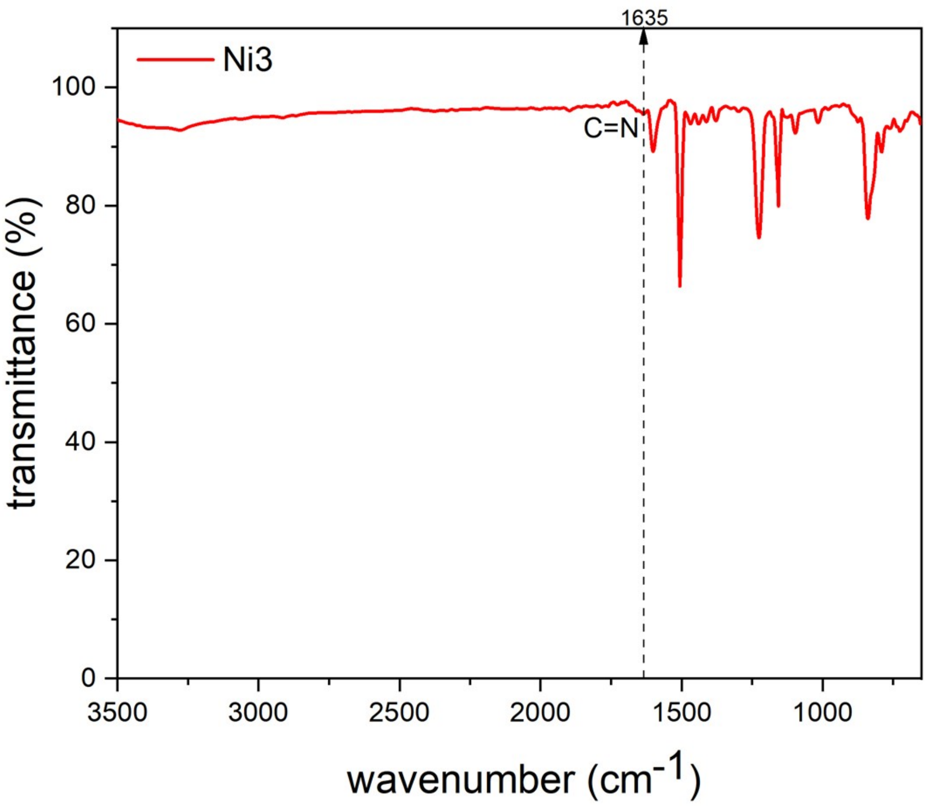

Figure S18 FT-IR spectrum of **Ni3**

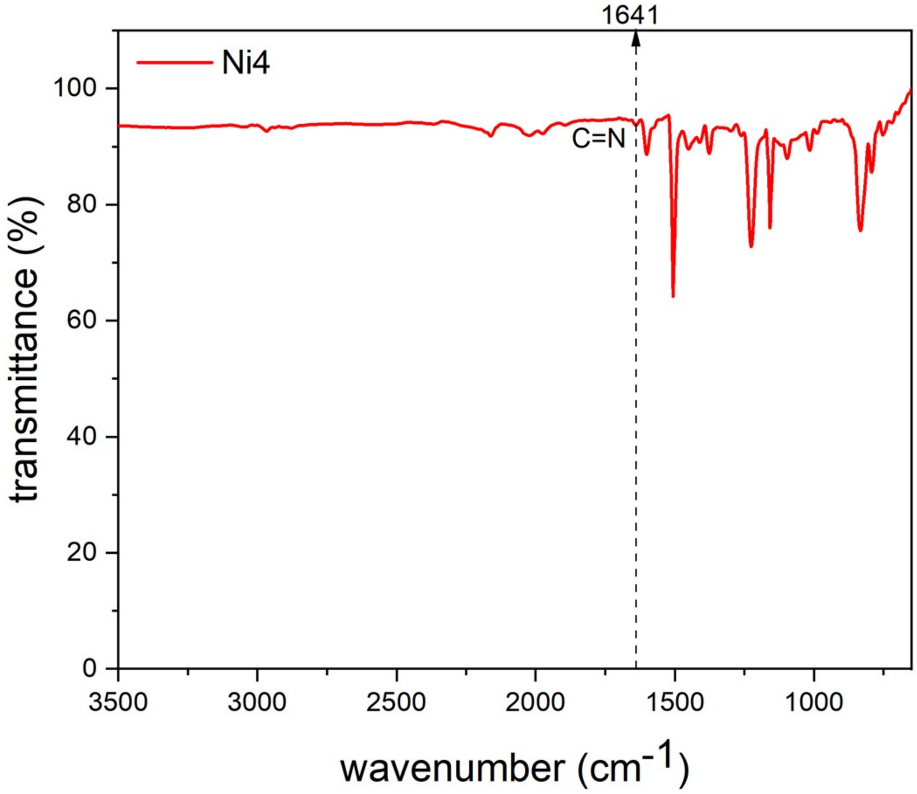

Figure S19 FT-IR spectrum of **Ni4**

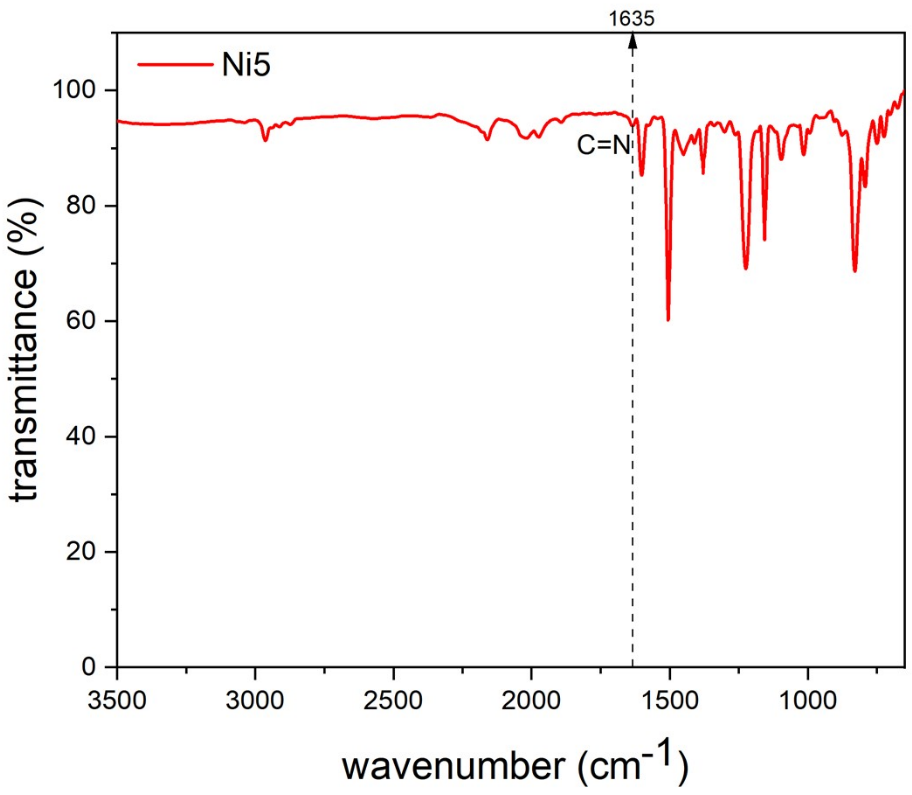

Figure S20 FT-IR spectrum of **Ni5**

^{1}H NMR (470 MHz, $CDCl_3$, 25 °C) spectra

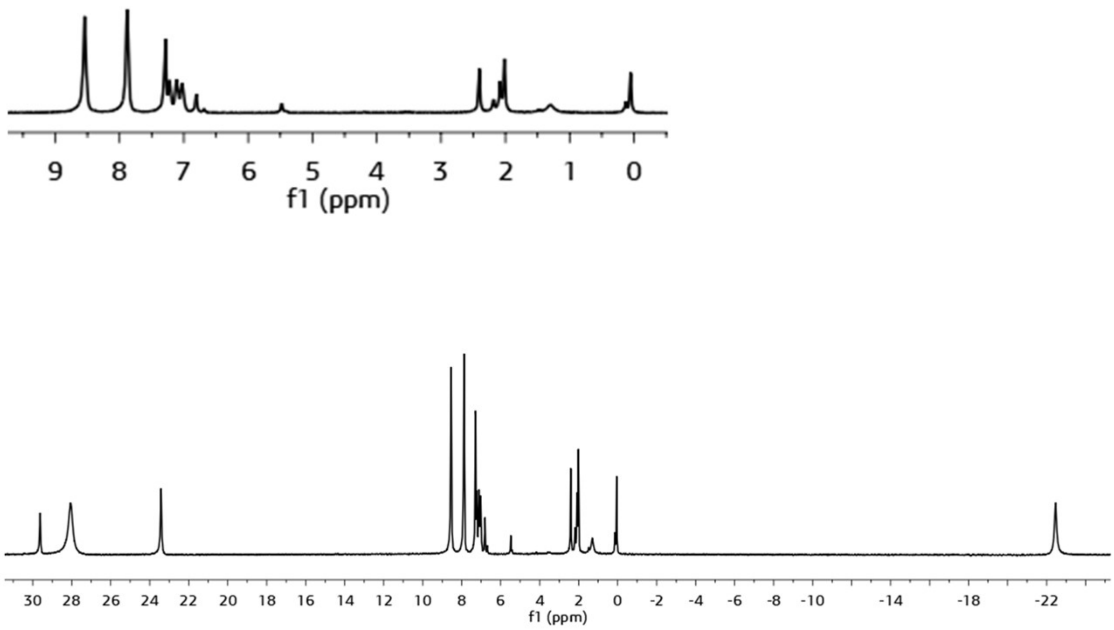

Figure S21 ^{1}H NMR spectrum of **Ni1** along with an expansion of the δ 10.0 to 0.0 ppm region

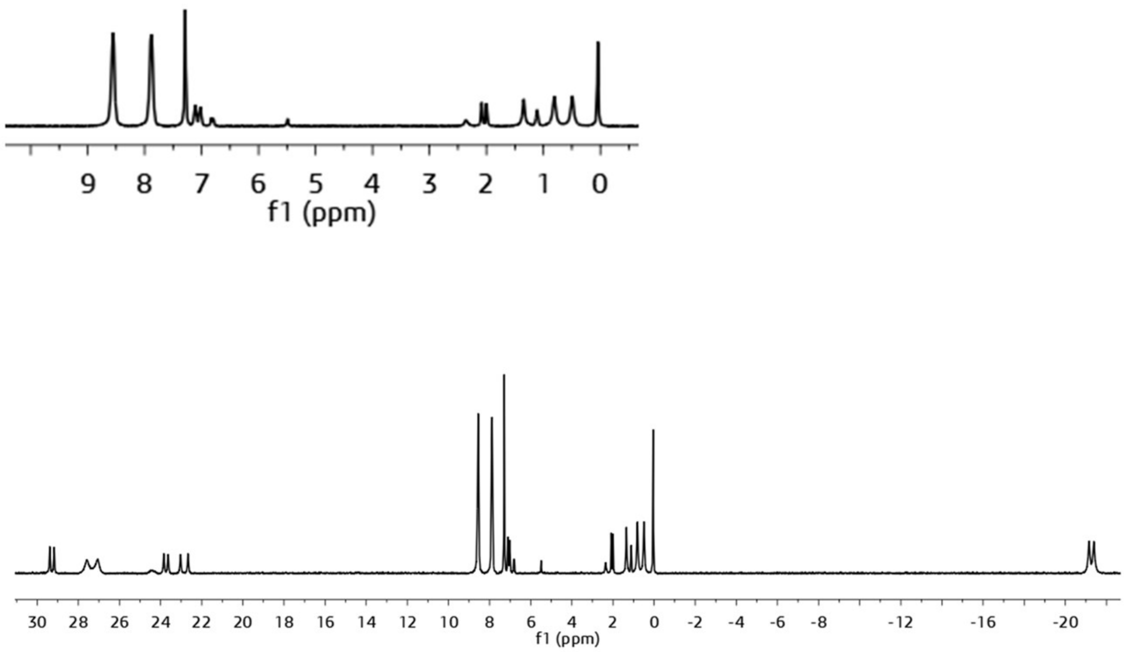

Figure S22 ^{1}H NMR spectrum of **Ni2** along with an expansion of the δ 10.0 to 0.0 ppm region

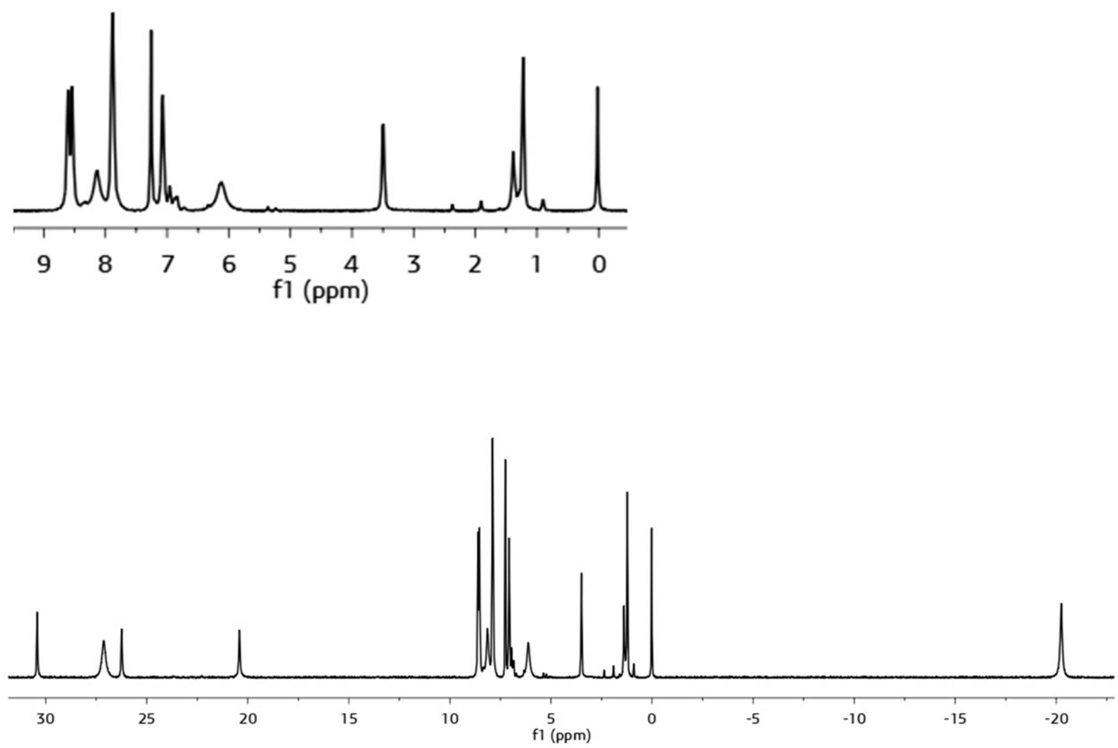

Figure S23 ^{1}H NMR spectrum of **Ni3** along with an expansion of the δ 10.0 to 0.0 ppm region

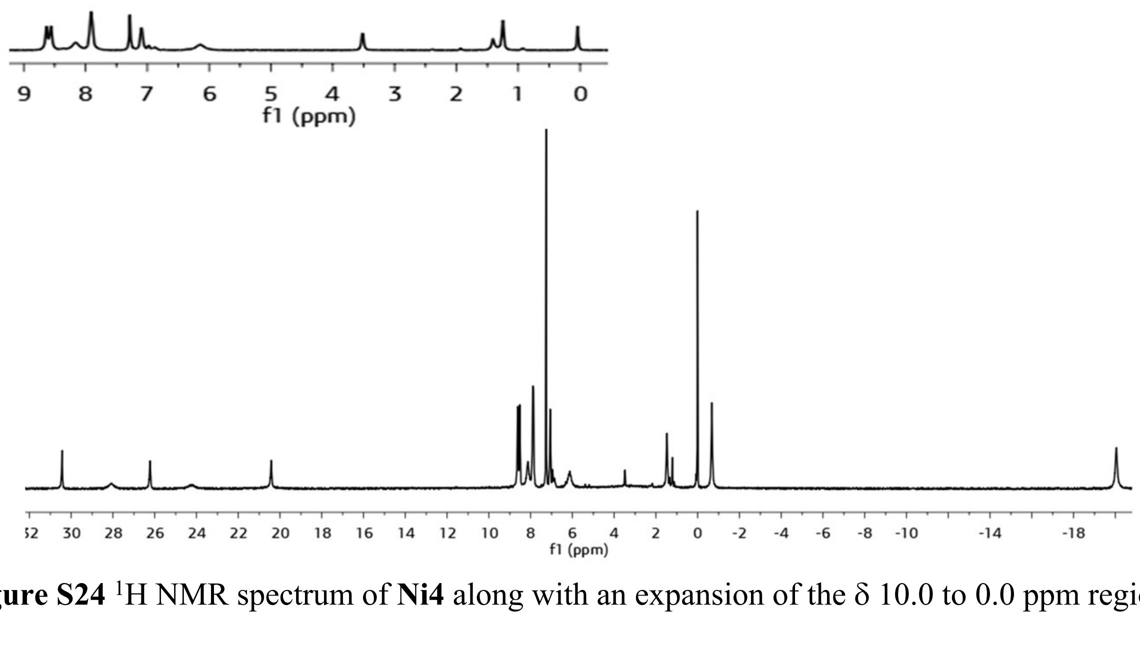

Figure S24 ^{1}H NMR spectrum of **Ni4** along with an expansion of the δ 10.0 to 0.0 ppm region

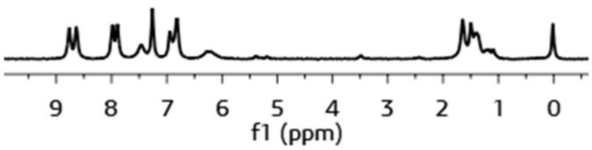

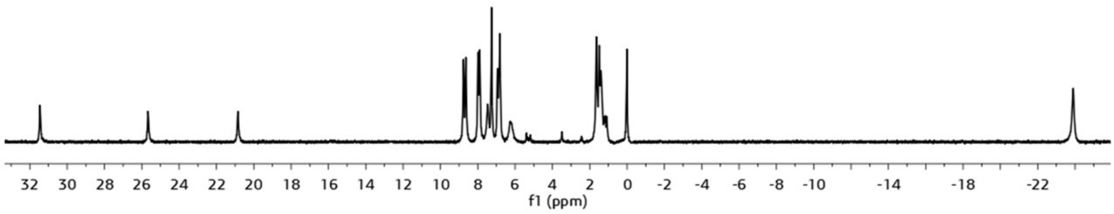

Figure S25 ^{1}H NMR spectrum of **Ni5** along with an expansion of the δ 10.0 to 0.0 ppm region

^{19}F NMR (470 MHz, $CDCl_3$, 25 °C) spectra

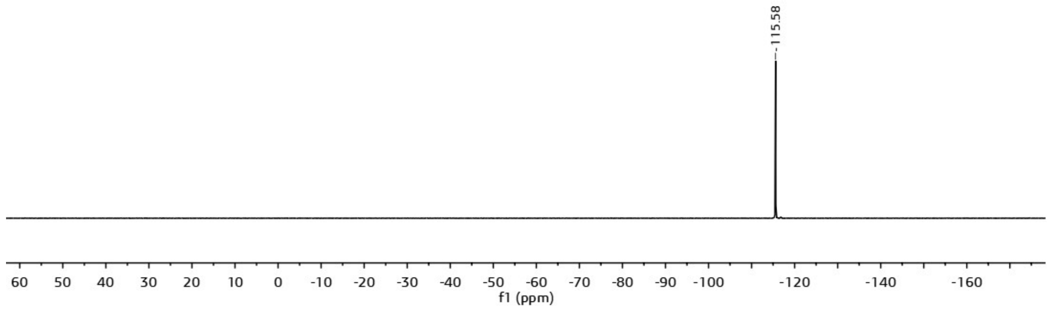

Figure S26 ^{19}F NMR spectrum of **Ni1**

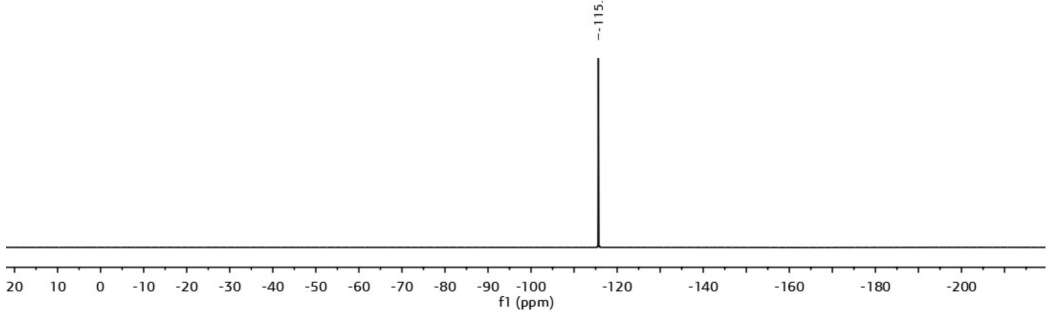

Figure S27 ^{19}F NMR spectrum of **Ni2**

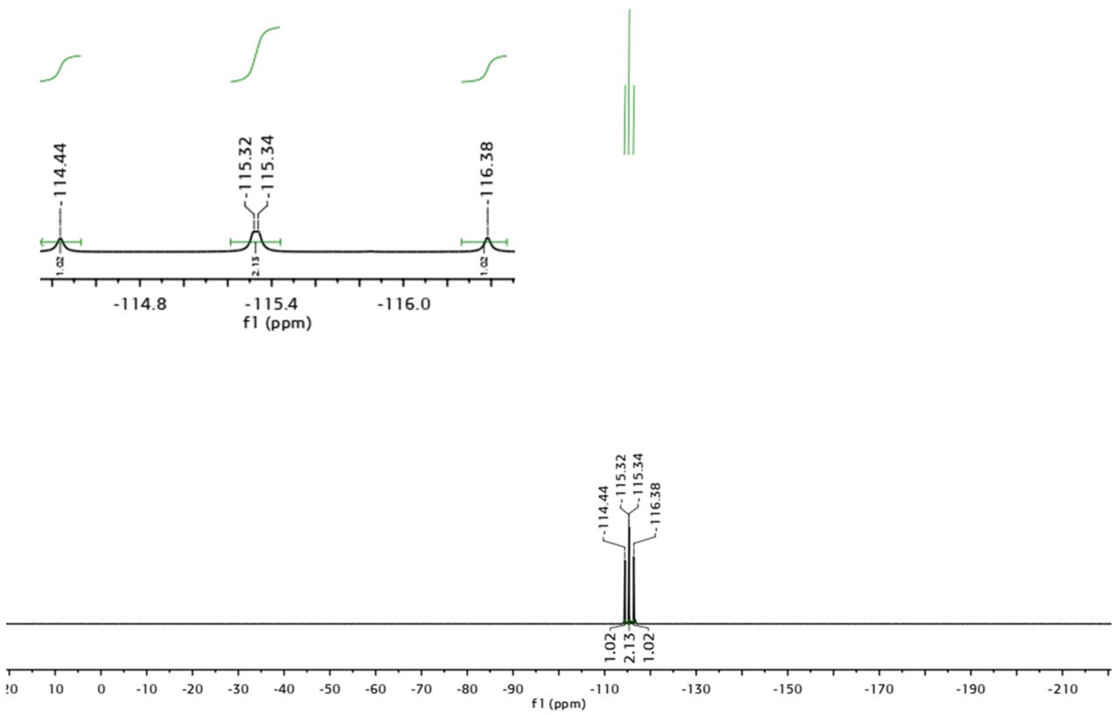

Figure S28 ^{19}F NMR spectrum of **Ni3**

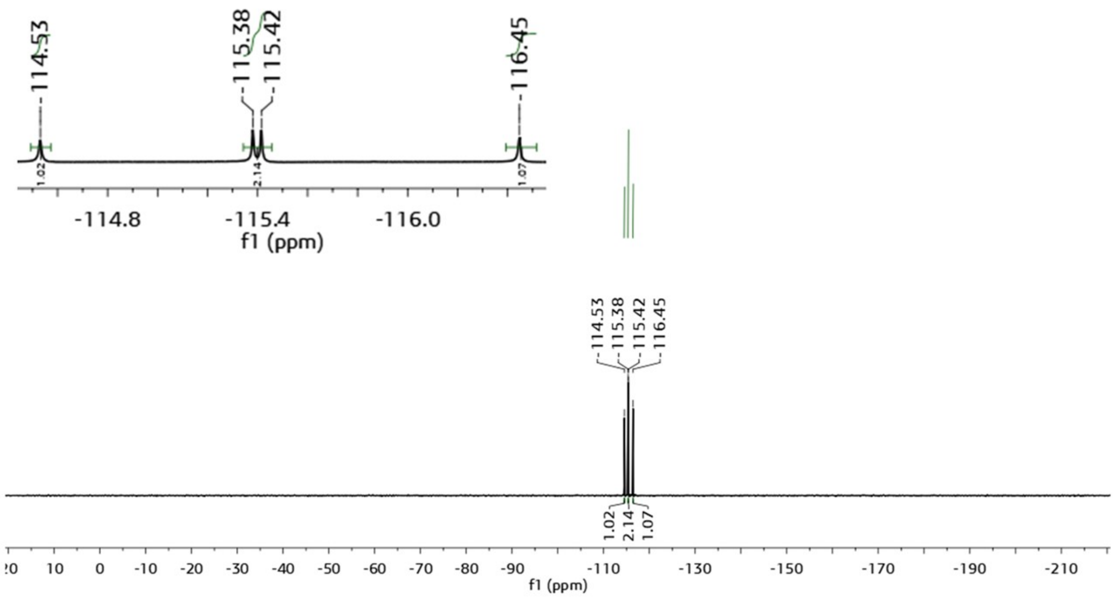

Figure S29 ^{19}F NMR spectrum of **Ni4**

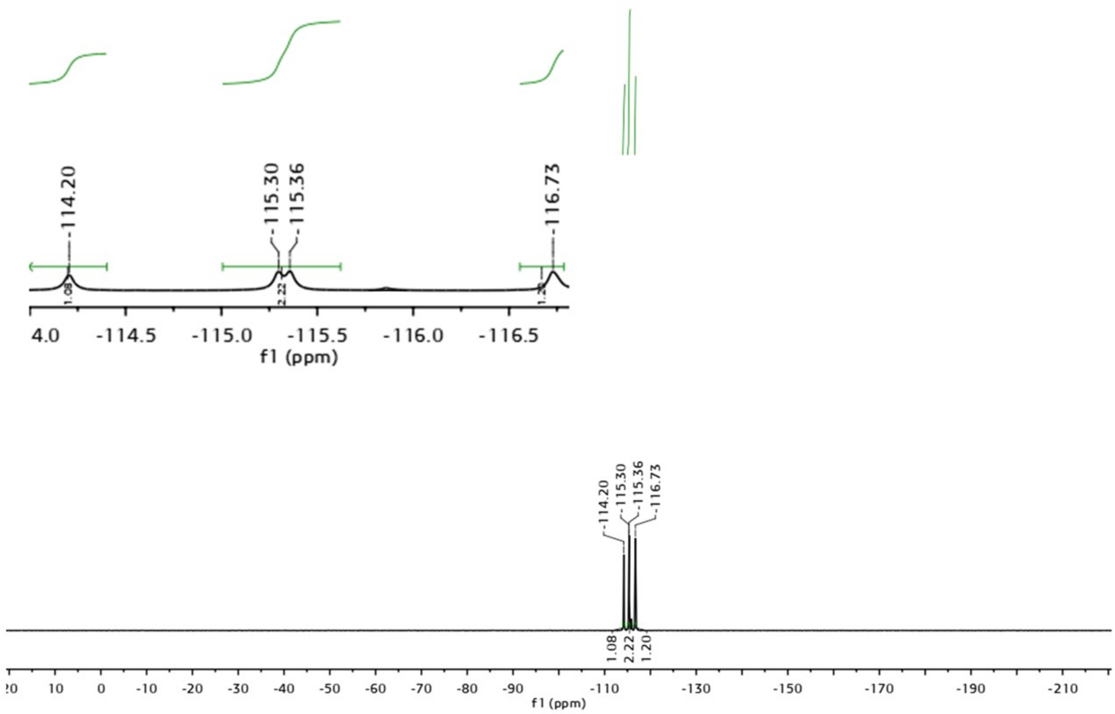

Figure S30 ^{19}F NMR spectrum of **Ni5**

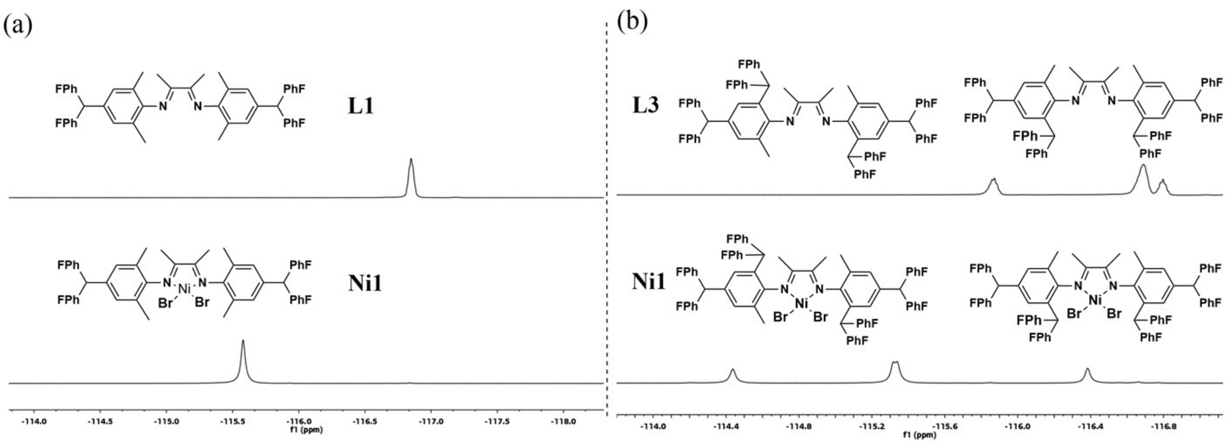

Figure S31 ^{19}F NMR spectra of a) **L1** and its nickel complex **Ni1** along with that for b) **L3** and **Ni3**.

GPC traces for the polyethylenes

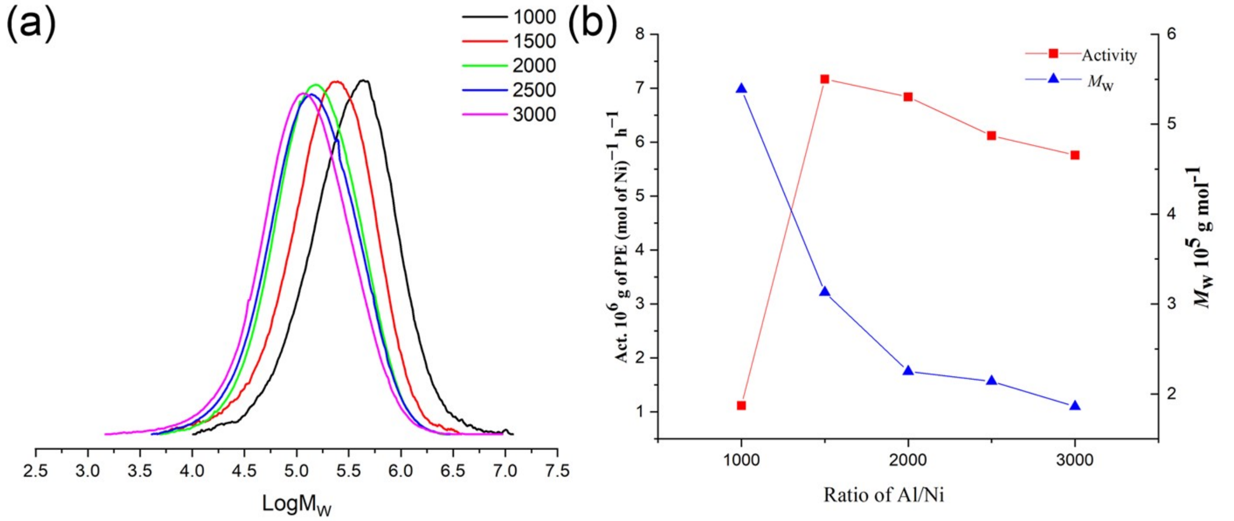

Figure S32 a) GPC traces and b) plots of catalytic activity and molecular weight of the polyethylene produced using **Ni2**/MAO at different Al:Ni molar ratios (entries 1 – 5, Table 3).

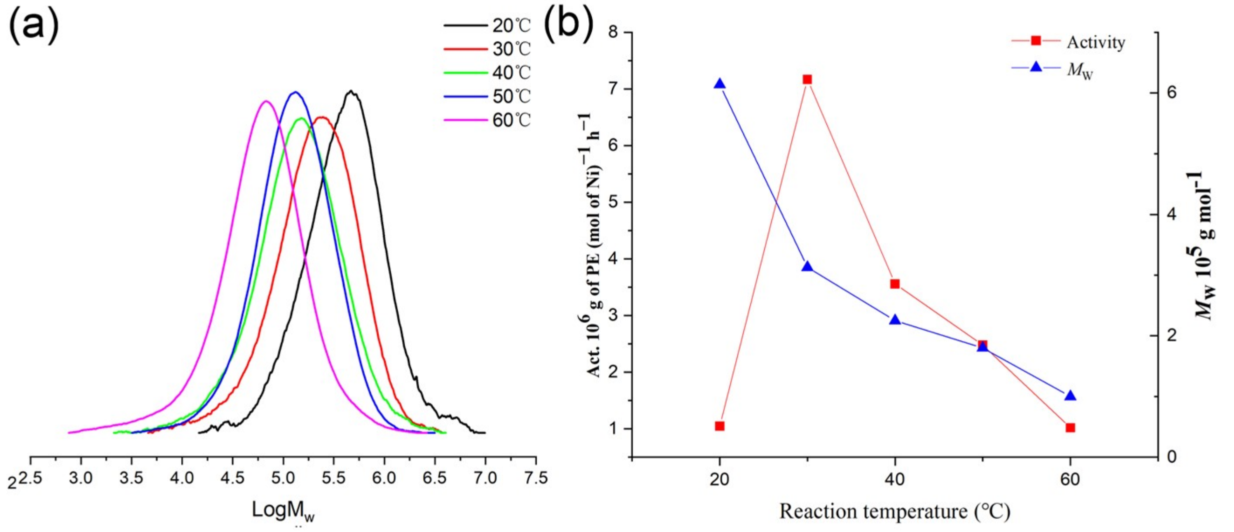

Figure S33 a) GPC traces and b) plots of catalytic activity and molecular weight of the polyethylene produced using **Ni2**/MAO at various run temperatures (entries 2 and 6 – 9, Table 3).

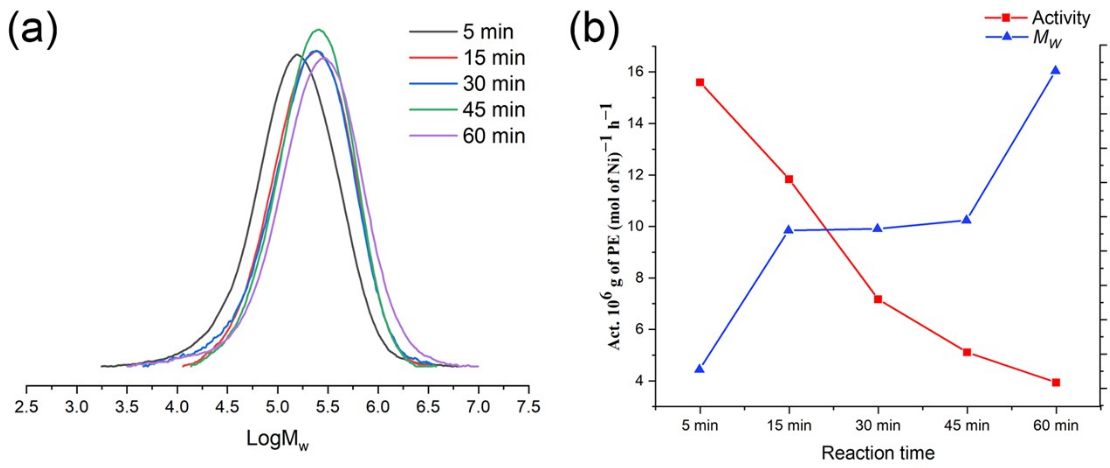

Figure S34 a) GPC traces and b) plots of catalytic activity and molecular weight of the polyethylene produced using **Ni2**/MAO at various time (entries 2 and 10-13, Table 3).

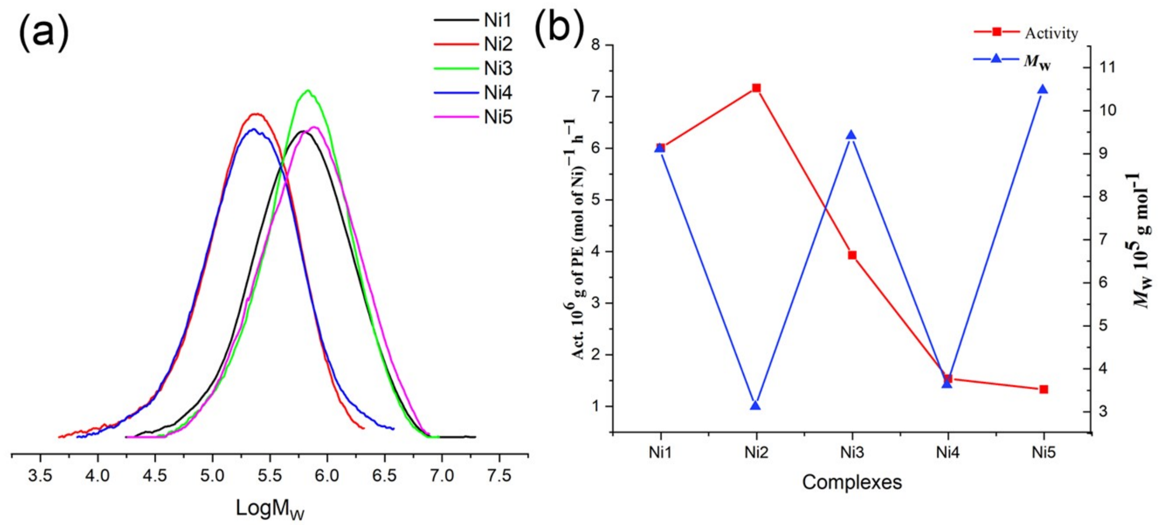

Figure S35 a) GPC traces and b) plots of catalytic activity and molecular weight of the polyethylene produced using **Ni1** – **Ni5** in combination with MAO (entries 2 and 16 – 19, Table 3).

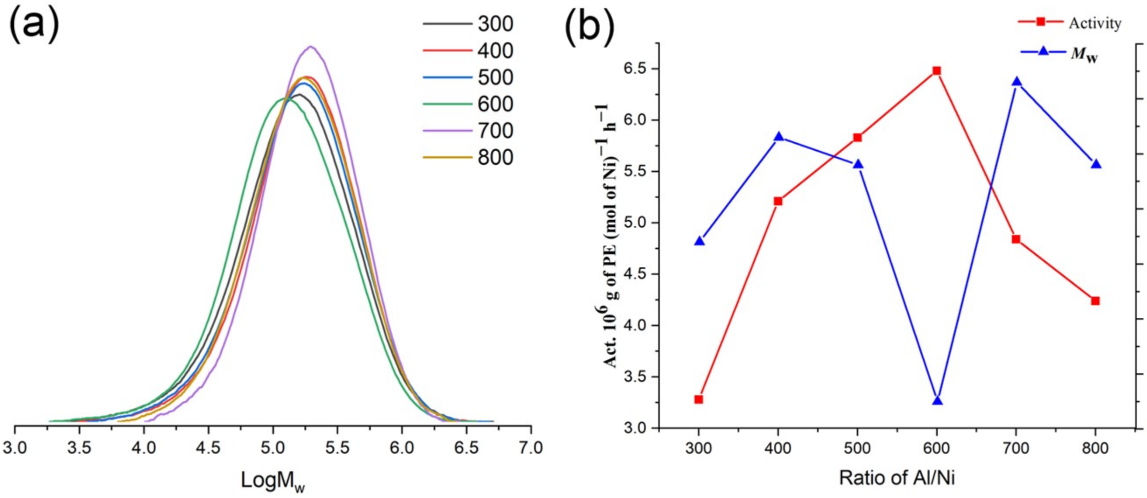

Figure S36 a) GPC traces and b) plots of catalytic activity and molecular weight of the polyethylene produced using **Ni2**/ $EtAlCl_2$ at different Al:Ni molar ratios (entries 1-6, Table 4)

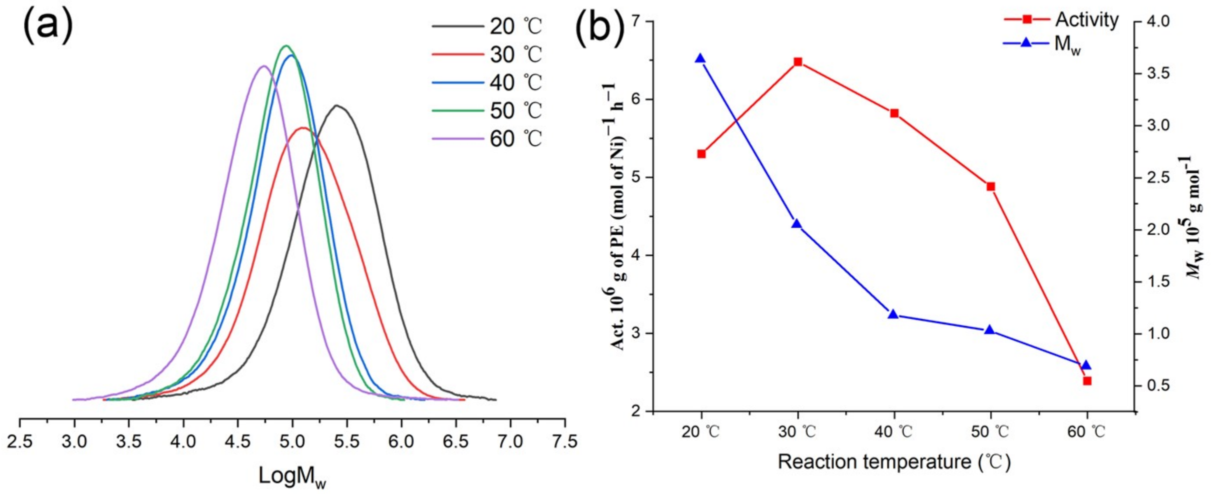

Figure S37 a) GPC traces and b) plots of catalytic activity and molecular weight of the polyethylene produced using **Ni2**/ $EtAlCl_2$ at different run temperatures (entries 4 and 7-10, Table4)

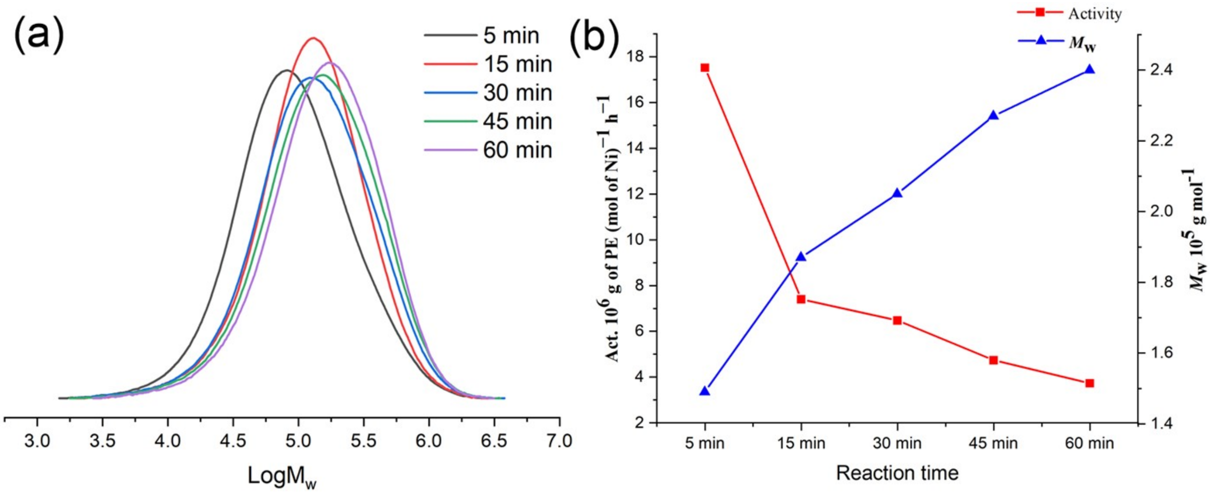

Figure S38 a) GPC traces and b) plots of catalytic activity and molecular weight of the polyethylene produced using **Ni2**/ $EtAlCl_2$ at different run time (entries 4 and 7-10, Table4)

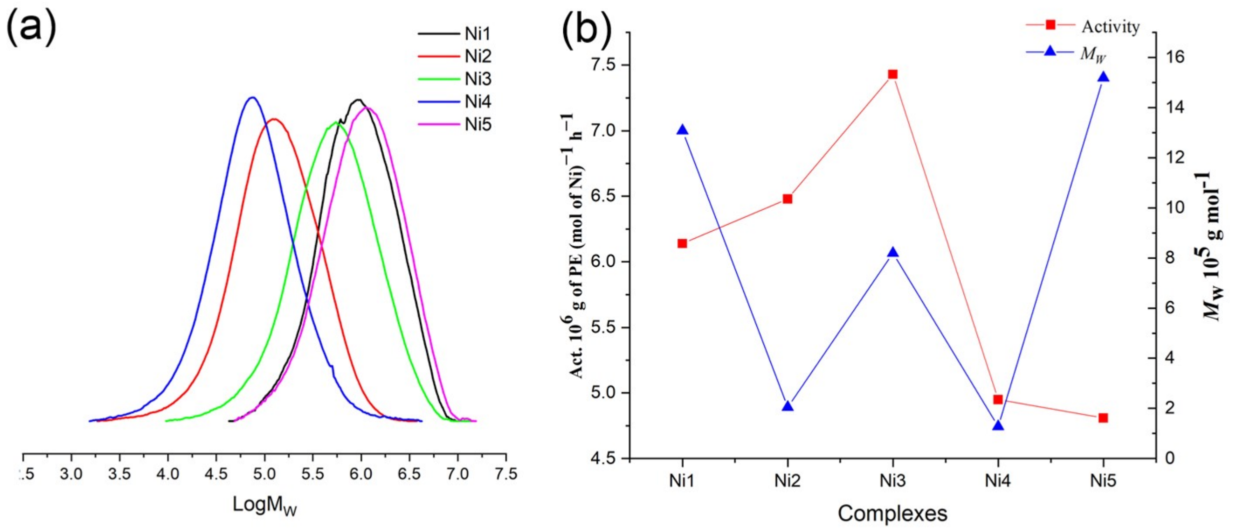

Figure S39 a) GPC traces and b) plots of the catalytic activity and molecular weight of the polyethylene produced using **Ni1** – **Ni5** in combination with $EtAlCl_2$ (entries 2 and 17 – 20, Table 4).

<u>^{13}C NMR (470 MHz, chlorobenzene-*d$_5$*, 100 °C) spectra</u>

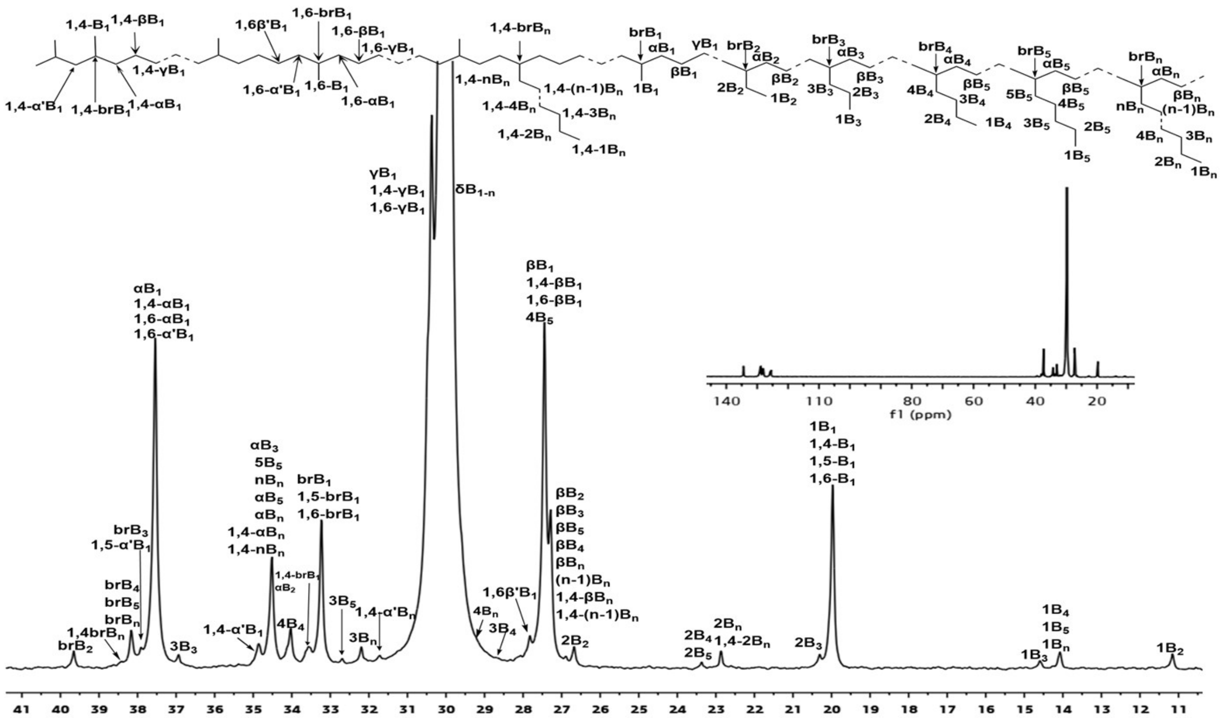

Figure S40 ^{13}C NMR spectrum of PE-MAO30Ni2 produced using **Ni2**/MAO (entry 2, Table 3)

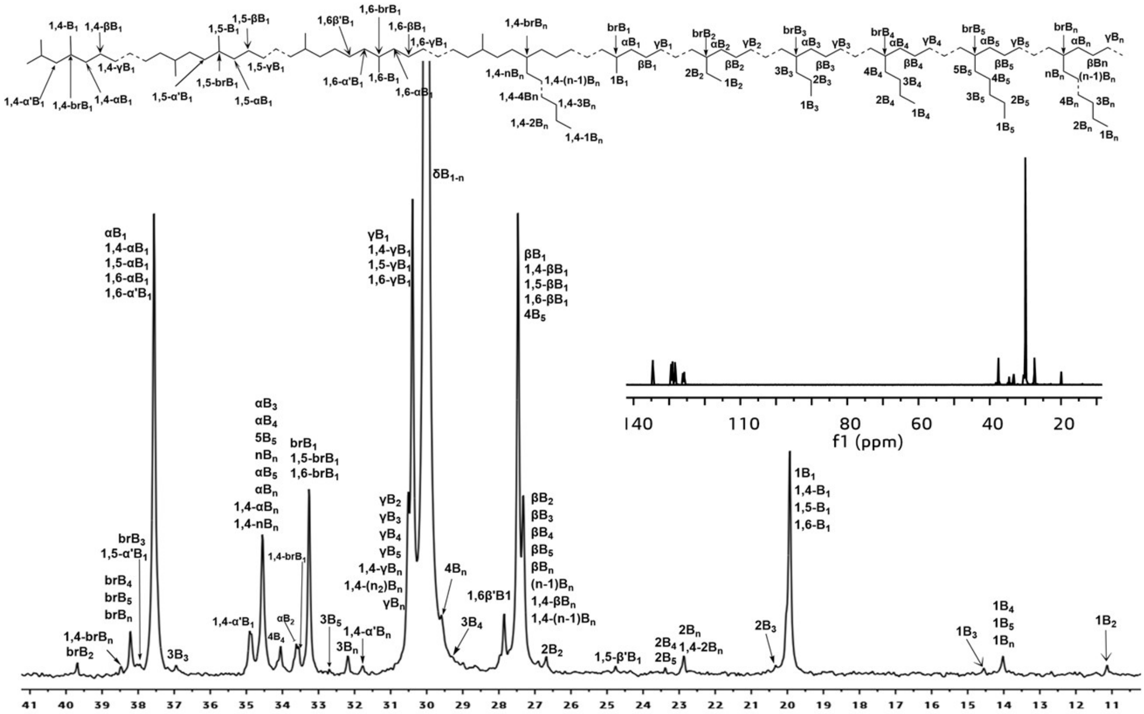

Figure S41 ^{13}C NMR spectrum of PE-EtAlCl$_2$40Ni5 produced using **Ni5**/EtAlCl$_2$ (entry 21, Table 4)

<u>^{13}C NMR (470 MHz, *o*-dichlorobenzene-*d$_4$*, 100 °C) spectra</u>

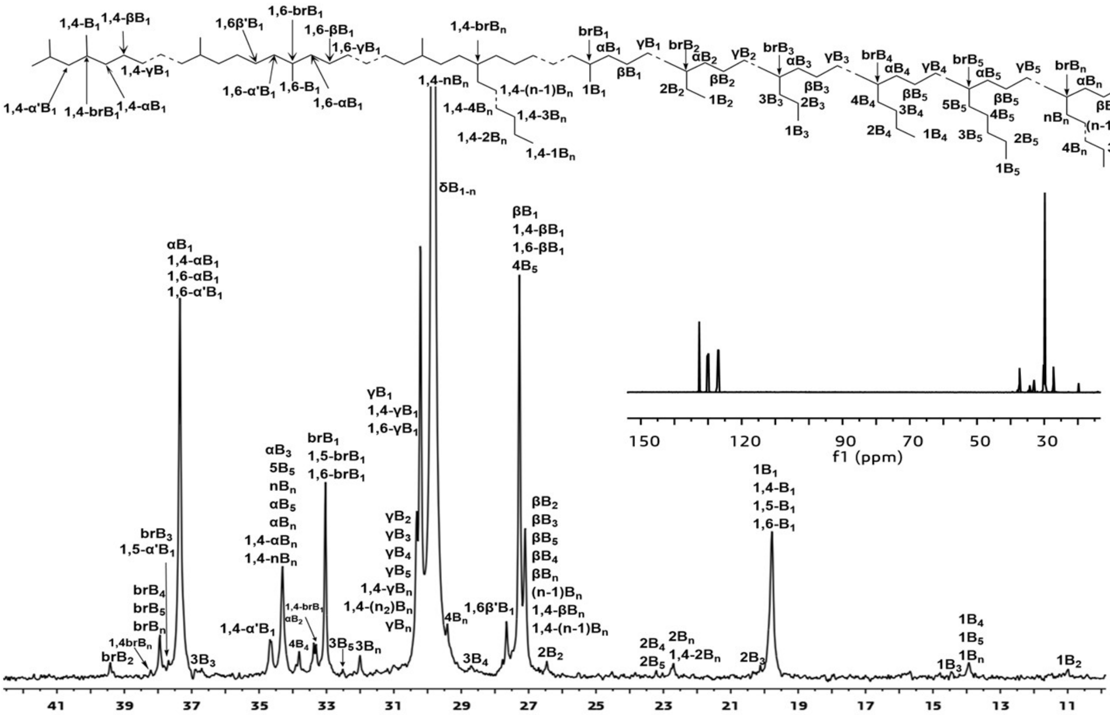

Figure S42 [13]C NMR spectrum of PE-Et_2AlCl40Ni5 produced using **Ni5**/Et_2AlCl (entry 23, Table 4)

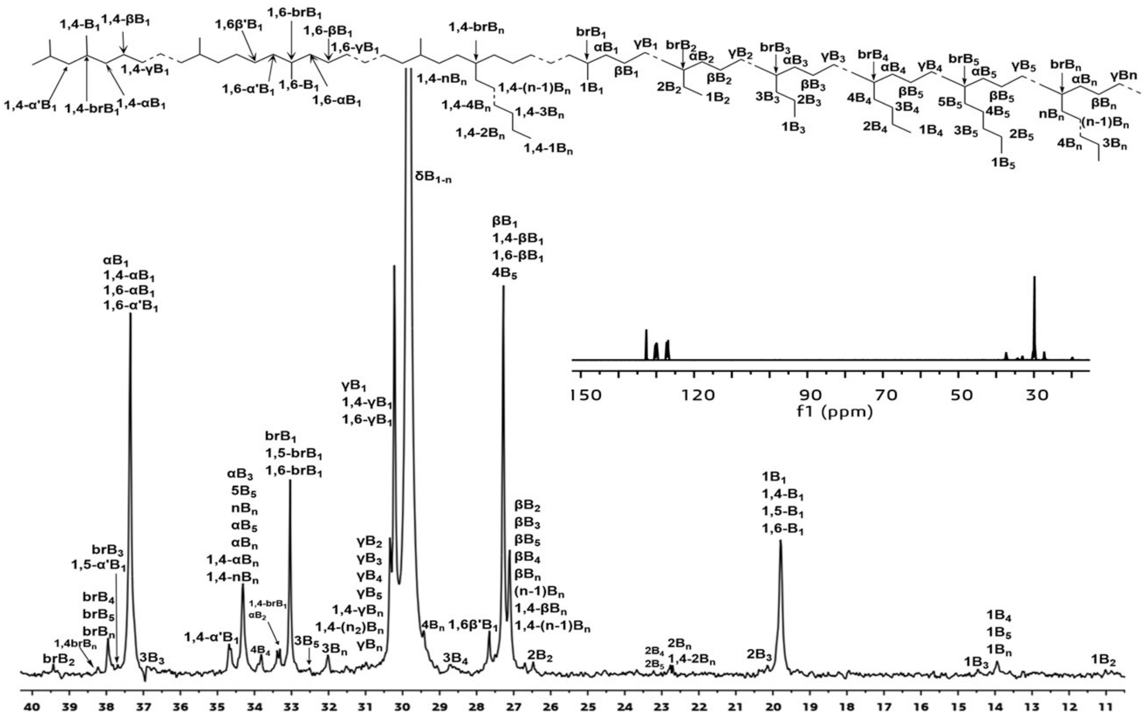

Figure S43 [13]C NMR spectrum of PE-EASC40Ni5 produced using **Ni5**/EASC (entry 24, Table4)

Stress-strain recovery test (performed at 30 ^{o}C)

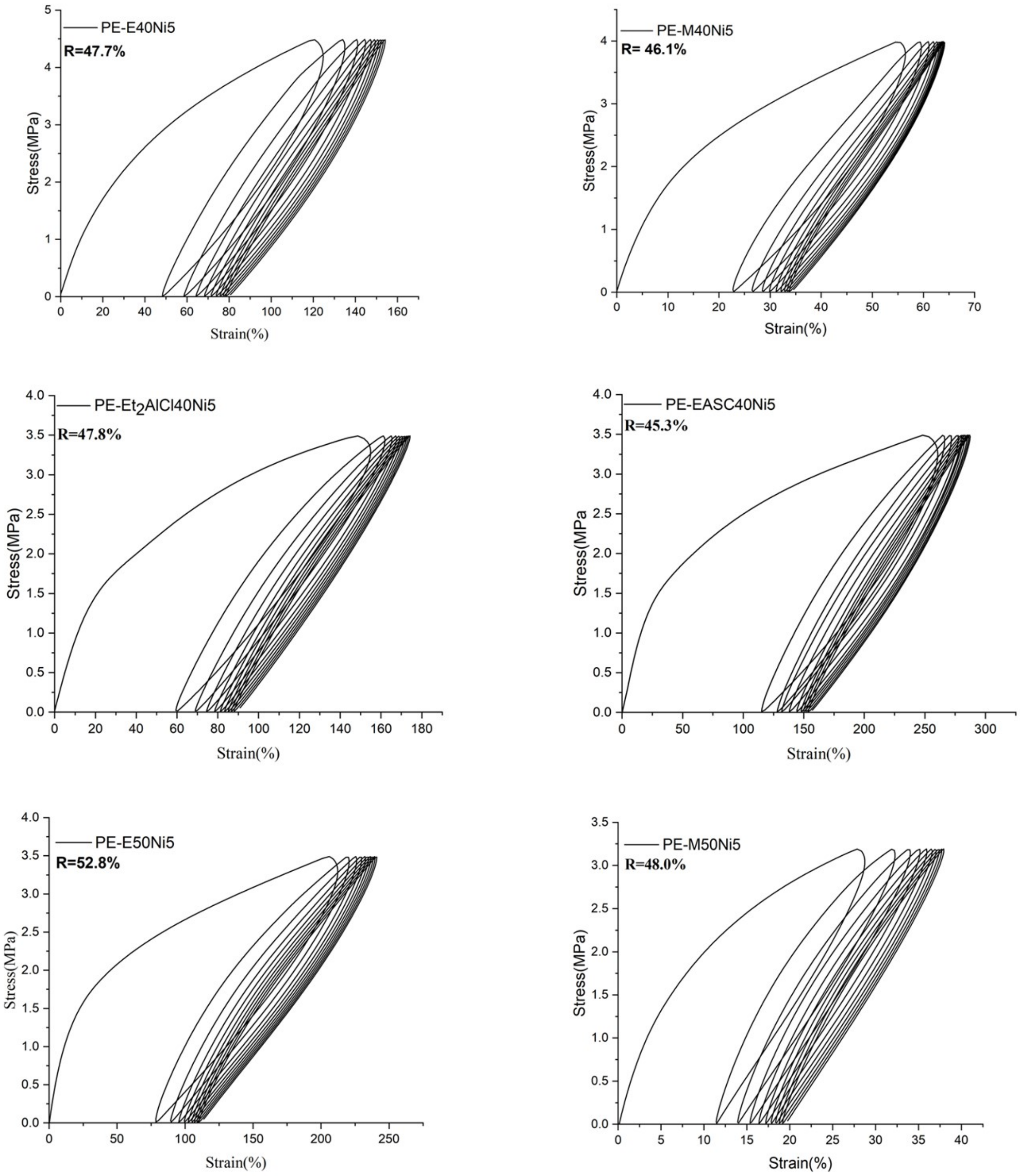

Figure S44 Stress-strain recovery tests for samples PE-EtAlCl$_2$40Ni5, PE-EtAlCl$_2$50Ni5, PE-M40Ni5, PE-Et$_2$AlCl40Ni5 and PE-EASC40Ni5

Table S1 Crystal data and structure refinements for **L3**, **Ni1** and **Ni5**			
	Ni1	**Ni5**	**L1**
Empirical formula	$C_{210}H_{156}F_{24}N_6$	$C_{92}H_{81}Br_4F_8N_4Ni_2$	$C_{74}H_{60}Br_2F_8N_2Ni$
Formula weight	3219.40	1831.67	1347.77
Temperature/K	170.00(10)	170.00(13)	169.99(12)
Crystal system	triclinic	triclinic	monoclinic
Space group	P-1	P-1	$P2_1/n$
a/Å	11.08370(10)	15.1623(12)	10.8443(4)
b/Å	19.80860(10)	15.6426(9)	36.4718(12)
c/Å	37.8410(3)	18.6622(9)	16.3540(7)
α/°	89.0030(10)	78.343(4)	90
β/°	84.9140(10)	78.089(5)	106.635(4)
γ/°	83.4140(10)	78.104(6)	90
Volume/Å^3	8220.55(11)	4178.7(5)	6197.5(4)
Z	2	2	4
ρ_{calc}g/cm^3	1.301	1.456	1.444
μ/mm^{-1}	0.778	3.337	2.542
F(000)	3348.0	1858.0	2752.0
Crystal size/mm^3	0.2 × 0.15 × 0.1	0.1 × 0.05 × 0.02	0.3 × 0.1 × 0.02
Radiation	Cu Kα (λ = 1.54184)	Cu Kα (λ = 1.54184)	Cu Kα (λ = 1.54184)
2Θ range for data collection/°	4.49 to 150.728	4.908 to 133.2	4.846 to 151.324
Index ranges	-13 ≤ h ≤ 13, -24 ≤ k ≤ 24, -47 ≤ l ≤ 41	-18 ≤ h ≤ 18, -18 ≤ k ≤ 18, -22 ≤ l ≤ 22	-12 ≤ h ≤ 13, -32 ≤ k ≤ 44, -20 ≤ l ≤ 20
Reflections collected	120556	55023	46177
Independent reflections	32478 [R_{int} = 0.0293, R_{sigma} = 0.0299]	14739 [R_{int} = 0.1001, R_{sigma} = 0.0840]	12209 [R_{int} = 0.1010, R_{sigma} = 0.0654]
Data/restraints/parameters	32478/0/2173	14739/1068/1200	12209/0/790
Goodness-of-fit on F^2	1.281	1.344	0.998
Final R indexes [I>=2σ (I)]	R_1 = 0.1097, wR_2 = 0.2897	R_1 = 0.1352, wR_2 =0.3446	R_1 = 0.1343, wR_2 =0.3939
Final R indexes [all data]	R_1 = 0.1223, wR_2 = 0.3090	R_1 = 0.1802, wR_2 =0.3816	R_1 = 0.1634, wR_2 =0.4189
Largest diff. peak/hole / e Å^{-3}	1.37/-0.55	2.88/-0.96	3.39/-1.02